Thermal Science and Engineering Progress 51 (2024) 102606

Contents lists available at ScienceDirect

Thermal Science and Engineering Progress

journal homepage: www.sciencedirect.com/journal/thermal-science-and-engineering-progress

# Heat transfer optimisation using novel biomorphic pin-fin heat sinks: An integrated approach via design for manufacturing, numerical simulation, and machine learning

Mohammad Harris [a,*], Hongwei Wu [a,*], Anastasia Angelopoulou [b], Wenbin Zhang [c], Zhuohuan Hu [d], Yongqi Xie [e]

[a] School of Physics, Engineering and Computer Science, University of Hertfordshire, College Lane Campus, Hatfield AL10 9AB, UK
[b] School of Computer Science and Engineering, University of Westminster, 115 New Cavendish Street, London W1W 6UW, UK
[c] School of Science & Technology, Nottingham Trent University, Clifton Lane, Clifton, Nottingham NG11 8NS, UK
[d] School of Energy and Power Engineering, University of Shanghai for Science and Technology, Shanghai 200093, China
[e] School of Aeronautic Science and Engineering, Beihang University, Beijing 100191, China

ARTICLE INFO

*Keywords:*
Heat transfer enhancement
Biomorphic pin fins
Mini and microchannels
Machine learning
Numerical simulation

ABSTRACT

With the availability of advanced manufacturing techniques, non-conventional shapes and bio-inspired/biomorphic designs have shown to provide more efficient heat transfer. Consequently, this research investigates the heat transfer performance and fluid flow characteristics of novel biomorphic scutoid pin fins with varying volumes and top geometries. Numerical simulations were conducted using four hybrid designs for Reynolds Number 5500–13500. The impact of pin fin 'top' geometrical features on the heat transfer coefficient (HTC) was evaluated by combining computational fluid dynamics (CFD), experimental data, and machine learning. The results highlighted that the new pin fins saved 6.3 % to 14.3 % volume/material usage but produced around 1.5 to 1.7 times more heat transfer than conventional square/rectangular fins. Also, manipulating pin fins via the top geometrical properties can lead to more uniform velocity and temperature distributions while demonstrating the potential for increased thermal efficiency with reduced thermal resistance. Furthermore, six machine learning models accurately predict HTC using volume and surface area as key variables, achieving less than 5 % mean absolute percentage error (MAPE). Overall, this research introduces innovative biomorphic designs with unconventional geometries, emphasising resource optimisation and efficient HTC prediction using machine learning. It simplifies design processes, supports agile product development, calls for re-evaluation of conventional heat sink geometries, and provides promising directions for future research.

## Nomenclature

| | |
|---|---|
| ***Latin Symbols*** | |
| A | Area,$m^2$ |
| Cp | Specific heat capacity,J/kgÂ·K |
| D | Diameter,m |
| Dh | Hydraulic diameter,m |
| h | Heat transfer coefficient,$W/m^2K$ |
| H | Height, m |
| K | Thermal conductivity,W/mÂ·K |
| L | Length,m |
| $\dot{m}$ | Mass flow rate,kg/s |
| Nu | Nusselt number, no unit |

(*continued on next column*)

**Nomenclature** (*continued*)

| | |
|---|---|
| $\dot{Q}$ | Heat energy rate,$W/m^2$ |
| R | Thermal resistance, K/W |
| Re | Reynolds number, no unit |
| SA | Surface area, $m^2$ |
| T | Temperature,C |
| U,V,W | Dimensionless parameter |
| u,v,w | Directional velocity,m/s |
| V | Volume,$m^3$ |
| W | Width,m |
| x,y,z | Directional vectors |
| X,Y,Z | Dimensionless parameter |
| ***Greek Symbols*** | |
| η | Efficiency, dimensionless |

(*continued on next page*)

* Corresponding authors.
*E-mail addresses:* m.harris8@herts.ac.uk (M. Harris), h.wu6@herts.ac.uk (H. Wu).

https://doi.org/10.1016/j.tsep.2024.102606
Received 10 February 2024; Received in revised form 8 April 2024; Accepted 29 April 2024
Available online 1 May 2024

**Nomenclature** (*continued*)

| | |
|---|---|
| ϵ | Epsilon |
| μ | Fluid viscosity, kg/m • s |
| ρ | Fluid density, kg/m$^3$ |
| δ | Rate of change |
| ***Subscripts/Superscripts*** | |
| a | air |
| b | base |
| bc | base case |
| f | fluid |
| F | fin |
| in | inlet |
| nc | new case |
| o | outlet |
| s | surface |
| th | thermal |
| ***Abbreviations*** | |
| CFD | Computational Fluid Dynamics |
| CT | Conical Top |
| DT | Diamond/tetrahedral Top |
| DV | Dependent Variable |
| FE | Fin Efficiency |
| GBR | Gradient Boosting Regression |
| HTC | Heat Transfer Coefficient |
| IV | Independent Variable |
| KNN | K-nearest Neighbours |
| MAPE | Mean Absolute Percentage Error |
| MLR | Multiple Linear Regression |
| MT | Mushroom/hexaprism Top |
| PIF | Performance Improvement Factor |
| PHT | Plain Hexagon Top |
| RF | Random Forest |
| RMSE | Root Mean Squared Error |
| SPF | Square Pin Fin |
| TED | Turbulent Eddy Dissipation |
| TKE | Turbulent Kinetic Energy |

## 1. Introduction

The miniaturisation of electronic gadgets has revolutionised the contemporary electronics industry, producing more powerful and portable devices than ever before. However, this progress during the fourth industrial revolution has triggered new challenges in the form of increased heat build-up inside densely packed electronic devices/components. Consequently, this heat build-up causes performance issues and can even damage internal components [1], making thermal management solutions an integral part of current research topics relating to sustainability. Effective thermal management strategies are crucial, as poorly managed heat systems lead to decreased device lifespan, wasted energy, and negative sustainable impacts [2]. Inadequate thermal management equally affects the overall performance of electronic devices, making them less efficient and unreliable [3].

The current challenge in electronic thermal management is to develop miniature heat transfer systems capable of dissipating heat quickly and effectively while maintaining the device's size and weight. To address these challenges, one promising solution that has gained significant interest is pin–fin-based heat sinks [4,5]. Heat sinks represent passive cooling methods that transfer heat from a heat-generating component (such as an electronic chip) to the surrounding air/fluid through a high-conductivity metal. Pin-fin heat sinks consist of small pins that increase the available surface area for heat transfer. By facilitating more efficient heat transfer through conduction, convection, and radiation, pin–fin heat sinks can cool electronic gadgets and extend their lifespan [6].

The recent extant literature trends highlight diverse experimental and numerical investigations to identify potential solutions to enhance fluid flow and heat transfer performance via pin–fin-based heat sinks; these methods include design modifications [6,7], surface modification [8], nanofluids [9,10], phase change materials [11], two-phase flows [12], inducing flow instabilities [13], amongst many other strategies [14]. Nonetheless, the literature indicates that design or geometrical adjustments mainly remain the focus. To illustrate, İzci et al. [15] numerically explored various single-arrangement pin-fins with shapes such as circular, square, diamond, triangular, cone, and rectangular fins. The results hinted that rectangular fin had the highest Nusselt Number (Nu) and friction factor, but the cone-shaped fins retained the highest thermal performance index. Also, inline-arrangement pin-fins having splitter plates with circular and square shapes have been numerically investigated by Razavi et al. [16] and Sajedi et al. [17]. They found that utilising splitters behind pin-fins reduces pressure drops and thermal resistance; this was more effective in circular shapes than square pin-fins. Similarly, the numerical assessment of inline circular pin-fins has been done many times [18–20]. It was observed that thermal performance has a positive relationship with the fin height but negative with the fin pitch; traditional setup of opposite positions of inlet and outlet have higher Nu and lower bottom temperature; the gap between the pin-fins and the sidewalls can manipulate heat transfer performance significantly.

Other investigations have analysed triangular [21,22], square [23], rectangular, diamond, oblong, elliptic [24], cones [25,26], hemispherical [27], alternative dimples [28], multi-bulges [29], micropillars [30], textured [31], curved/inclined [32], splitter inserts [33], and grooves [34–36]; it was noted that the porosity and the angle of the fins have a great impact on the thermal performance; diamond-shaped fins had higher Nu, rectangular-shaped had higher pressure drops, and adding splitters, deep grooves, domes, and increasing the circular diameter — whilst reducing the spacing between the fins — improves heat transfer. Additionally, experimental investigations on pin–fin heat sinks have been carried out; however, these are less common than numerical studies, primarily due to the costs and difficulties involved in producing microscale pin-fins and heat sinks. Experimental studies having pin-fins exist in conventional shapes such as circle [37–39], semi-circle [40], conical [41], square [42], diamond, triangle, pentagon, and hexagon [43].

For experimental studies, staggered layouts represent a typical strategy [41,44]. Staggered arrangement pin-fins show that shape affects the vortex resistance, with a circular shape having the maximum resistance and the oval fins maintaining the minimum; the highest heat transfer was present in the hexagonal cross-section; circular fins showed the lowest pressure drops; also, the porosity and fin diameter affects the heat transfer rate. Due to the comparatively lower availability and complexities associated experimental investigation, many numerical studies are cross validated using other similar experimental/numerical data [45]. For instance, Xie et al. [46] appraised thermal and hydraulic performances of microchannel pin–fin heat sinks using data from external investigations [47,48]. The results of Xie et al. highlighted that in-lined pin-fins at a 30° inclined angle increase secondary flow at the cost of increased friction, but a steeper inclined angle doesn't necessarily improve heat transfer; 0° inclined angle performs similarly to other conditions and switching from in-lined to staggered pin–fin arrangement had minimal impact on thermo-hydraulic performance; thus, the exact effects of staggered and inline pin–fin arrangements still needs a better understanding. Nonetheless, the staggered setup is generally more preferred [49,50].

Further appraising more designs, in addition to the conventional geometries, researchers have attempted to utilise non-conventional shapes [51] and experimented with wings [52], hydrofoil [53], non-linear fins [54], NACA aerofoil pin-fins [50,55–57], irregular polygon [58], branched and interrupted [59], U-turn hybrid fins [60], and twisted fins [61]. With the recent rise of additive manufacturing-based heat sinks, more complex shapes are being explored [62,63]. Most recently, Bhandari et al. produced a review of the effects of different common and some unconventional pin–fin shapes [64] Interestingly, bio-inspired structures and surface morphologies are also increasingly becoming popular in heat sinks; however, the availability of bio-inspired and biomorphic pin–fin heat sink research tends to be scarce; the term 'biomorphic' refers to designs that uses naturally occurring shapes and

patterns. Recent research suggests some implementation of piranha [65], mushroom-shaped [66], tree-shaped [67], petaloid and shark skin-inspired pin-fins [68]. The results related to bio-inspired pin-fins show superior performance over traditional shapes or geometries.

Nonetheless, from a design and optimisation perspective, the effectiveness of pin–fin-based heat sinks depends on several factors, including the heat sink design, working fluid, and the thermal conductivity of the materials. Additionally, pins-fin geometrical configurations, such as shape, spacing, and height, can affect the heat transfer rate or coefficient [45]. Thus, the optimal design of a heat sink needs consideration of the device's thermal load or heat flux, size, shape, and operating environmental conditions [8]. In addition, the fluid flow around heat sinks significantly impacts their cooling performance. Increasing the flow rate can enhance heat transfer by promoting convective cooling. However, high airflow rates can also increase noise levels, induce higher pressure drops, require large fans or pumping power, and ultimately affect the device's size and weight. As a result, achieving the optimum balance between cooling performance and other design considerations is critical [1].

Moreover, from a fabrication and replicability point of view, the material choice and fabrication methods dictate the heat sink's weight, cost, and manufacturability — therefore, the trade-off between these three elements needs adjustments based on the application [69]. Thus, despite their effectiveness, pin–fin-based heat sinks contain some limitations. One significant challenge is their manufacturing complexity, which can increase cost and limit scalability. The high aspect ratios of the pins or fins, along with their microscale geometry, make them challenging to fabricate; plus, the manufacturing process must ensure that the pin-fins are free from surface defects that could reduce their heat transfer effectiveness [70]. On top of that, pin–fin-based heat sinks need a comparatively large surface area to be effective, limiting their integration into some electronic devices with minimal space.

One a different note, as most previous research focuses on experimental and numerical validation based design optimisation, machine learning and artificial intelligence techniques are slowly becoming popular in heat sink-related research [71]. They provide a promising alternative for numerical simulations/validation and can even generate novel insights that might not have been possible previously. Thus, integrating the simulations/experiments with machine learning techniques can help expanding the current research space [72,73]. Nevertheless, machine learning research in thermal management and heat transfer related fields is still relatively new, and more efforts and investigations are warranted [74] to provide a holistic impact.

Therefore, heeding to the literature findings and assessing the current industrial needs, in this paper, novel bio-inspired pin–fin heat sinks are proposed — whilst integrating manufacturing considerations. The paper aims to provide the following major novel contributions: 1) design of a new type of hybrid pin-fins with non-conventional geometries that can be produced using additive manufacturing; this innovation could expand the current design space and offer advantages over traditional pin–fin designs. 2) appraisal of the effects of combined features with different pin–fin "top" geometries via numerical simulations to gain new insights into fluid flow and heat transfer characteristics, adding further domain knowledge to this area. 3) heat transfer performance optimisation via manipulating design properties that can lead to improved performance with reduced volume and material usage — whilst considering the trade-off between design complexity and performance. 4) propose a simplistic machine learning model to predict heat transfer and provide quick performance indicators and reduce design development and exploration times.

Consequently, to achieve the research aim, numerical simulations and external experimental data, machine learning strategies were utilised to improve designs and provide additional insights. The advantage of using non-conventional geometries help to not only understand the effects of novel geometries, but it also avoids data being overfitted to a certain type of designs, which is arguably often the case in existing research. Therefore, during this era of ever-changing technological and rapid advancements, following mixed methods, combining strategies, and technologically driven approaches can enable further scope for continuous improvement [75]; moreover, this investigation ties in with the bio-inspired design philosophy [76] and adds value-added contributions to this research field. Accordingly, this research revolves around its research aim and is structured into distinct sections. The first two sections evaluate current design trends and tactics to form the baseline for this study; the design analysis, machine learning predictions, and numerical CFD simulation of several pin–fin setups are highlighted in section 3 and 4; the latter chapters include critical analysis and conclusion.

## 2. Heat sink design

The use of air-cooled pin–fin heat sinks for electronic devices remains a research hotspot [7,77–79]. For heat transfer enhancement, it is necessary to increase the contact/surface area between the pin-fins and working fluid and induce flow disturbances—while minimising the resulting rise in flow resistance. Therefore, a trade-off of different parameters needs consideration depending on the type of application. Additionally, adhering to the design for manufacturing (DfM) philosophy, designs must be replicable with reduced cost, materials, and manufacturing complexities. Consequently, an additive manufacturing strategy is required to manufacture pin-fins with complex shapes but with a reduced volume of material to save manufacturing costs [62].

### 2.1. Biomorphic design for manufacturing (DfM) philosophy

Nature and organisms have developed various survival strategies and shapes to adapt to their environments. The authors' previous works briefly explored the thermodynamics and thermal performance of nature-inspired biomorphic pin–fin designs [66,80]. Therefore, adopting a similar biomorphic approach, which involves designing inspired by nature, organisms, or naturally occurring shapes, a shape existing in skin cells (Scutoid) [81] was used as a baseline to propose four new pin–fin structures. While skin cells are linked together for material delivery, the biomorphic analogy to skin cells emphasises the efficient utilisation of surface area and generating flow disturbances for enhanced heat transfer, rather than a direct imitation of their arrangement, which would be the case in biomimetic design philosophy and is outside the scope of this work.

Moreover, the pin–fin utilises two geometries in a unique shape; thus, there is scope to save materials in the new designs compared to the base fin design — whilst still producing the desired results. The proposed pin–fin structure consists of arrays of staggered pin-fins, in comparison to the in-lined base rectangular/square pin–fin design (SPF). The "top features" of the biomorphic pin–fin structures are designed with specific characteristics, such as sharp edges, faces, and curvatures, aimed at enhancing heat transfer, inducing flow disturbances, and manipulating the volume of material used in the design. In other words, the "top features" are engineered protrusions strategically placed on the pin–fin structures. The design philosophy behind these features involves manipulating their shape/dimensions for maximum effectiveness in heat transfer enhancement while considering the constraints of manufacturing feasibility and cost of material.

By aligning with DfM principles, the proposed pin–fin designs aim to strike a balance between enhanced heat transfer performance, reduced product development time, and practical manufacturing considerations of complex pin–fin geometries via additive manufacturing or metal 3D-printing; this holistic approach offers efficient and sustainable air-cooled pin–fin heat sinks. Furthermore, in the existing literature, hexagonal, pentagonal, twisted, protrusions, etc., have primarily been employed individually. Thus, one of the objectives of this study is to integrate various modifications to develop a hybrid pin–fin design and assess their combined effects to gain new insights into the underlying physics and

performance. Despite the potential benefits of similar design modifications for flow and thermal boundary layer manipulation, there have been limited studies on combining these distinct concepts/strategies within pin–fin heat sink investigations; hence, this makes the current investigation worthwhile. Fig. 1 displays the traditional base design featuring rectangular/square pin–fin designs (SPF) that is used for comparison and numerical validation purposes. Additionally, Fig. 1 includes a 3D-printed prototype representing the base geometry of the novel scutoid pin-fins for visualisation purposes of the physical model.

The new designs followed the same heat sink dimensions for the base design — such as the same internal fin occupied width ($Wb_i$), height of the base ($H_b$), source/heat flux height ($H_f$), etc. However, the new designs incorporated different shaped "top" features with a scutoid base geometry. Moreover, they vary in the surface area of the "top" geometry, aiming to manipulate the volume of materials used and comprehend the impact of different shapes. For detailed geometrical information, refer to Table 1, which outlines the dimensions of each design. The material usage (%M) shows the reduction of weight in comparison to the base design (SPF).

As mentioned in the earlier paragraphs, the base geometry of the pin-fins utilised a combination of pentagonal and hexagonal shapes to save materials and introduces twists to generate flow disturbances. Additionally, alterations in the top geometry enable the manipulation of boundary layers, providing insights into the flow characteristics of these novel shapes. Given that the proposed designs are intended for additive manufacturing, the critical goal is to save material/weight while ensuring efficient heat transfer. A reduced surface area hampers heat transfer, while an increased surface area adds more volume — contributing to higher material usage and costs. Therefore, the volume of the new pin-fins was constrained within a ±15 % range from the base design SPF to strike a balance between reduced material usage and increased heat transfer efficiency. Maintaining a ±15 % range in the volume of the new pin-fins relative to the SPF design ensures a reasonable degree of flexibility in design modifications without deviating significantly from the original parameters. Moreover, this range arguably aligns with industry standards and current engineering and design practices.

In the initial paragraphs, the existing literature suggested that hexagons, tetrahedrons, cones, and mushroom/prism shapes can enhance heat transfer. Consequently, a combination of various pin–fin strategies was investigated to get a more robust understanding of underlying flow characteristics and physical processes. While the PHT and DT designs focused on altering the flow through a change in the height of the top fins, the CT and MT designs elongated the lateral surfaces of the fins. The first PHT design featured a plain hexagon top with 5 % more pin height and 0.5 mm more side width than the other scutoid pin fins. This adjustment aimed to maintain the reduction in volume/surface area of PHT within the initially discussed ±15 % acceptable range. The plain surface of PHT could potentially enable boundary layer formations on top while inducing turbulence between and around the fins. All the other designs had 4.5 mm sides/60 mm fin height. However, there are minor variations between the spacing distances of the fins due to the difference in the fin-top geometry, to avoid interactions, and leave a reasonable amount of gap between the extended surfaces, especially for the CT and MT designs.

The second design, CT, featured a cone-shaped pointed top geometry, where the pointed shape was expected to cause flow separations, while the smooth surface of the cone can lead to flow attachments. The third design, DT, incorporated an extended tetrahedral diamond-shaped structure inside the top geometry of the fins, with sharp edges capable of generating turbulence. The last design, a sharp biomorphic mushroom-shaped prism, covered the top of the fins extensively in an attempt to increase the heat transfer area. In addition to these design modifications, there was a 90 degree twist and a vertex within the fin-base geometry converting the pentagonal shape into a hexagon and causing the designs to have a slight curve. Thus, all the combinations existing within these design modifications produced a new type of novel hybrid pin-fins. Despite the complexity of the pin–fin shapes, as illustrated in Fig. 1

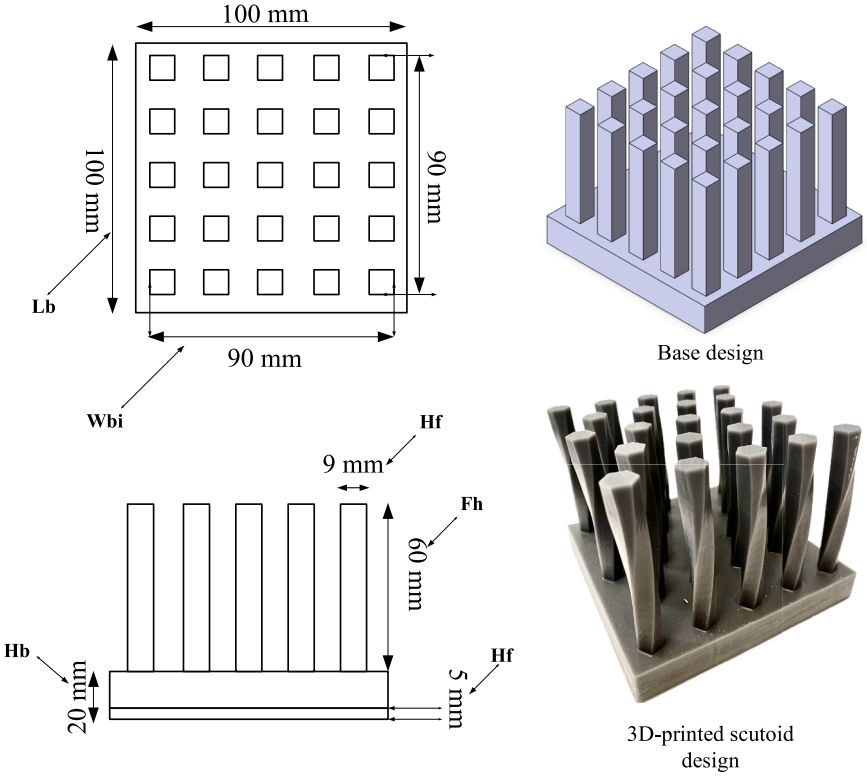


**Fig. 1.** Base design and 3D-printed new prototype design.

**Table 1**
Details of geometrical data for all designs.

| Model | Top-fin Geometry | Fin Height ($H_f, mm$) | No. of Fins ($N$) | Surface Area ($SA, m^2$) | Volume ($V, m^3$) | Mass ($M, g$) | Material (%M) |
|---|---|---|---|---|---|---|---|
| SPF | Square | 60 | 25 | 80,000 | 271,500 | 271.5 | – |
| PHT | Hexagon | 63 | 23 | 70,646 | 232,542 | 232.5 | −14 % |
| CT | Cone | 60 | 23 | 73,540 | 250,542 | 250.5 | −8% |
| DT | Tetrahedral | 60 | 23 | 71,590 | 245,093 | 245.1 | −10 % |
| MT | Hexaprism | 60 | 23 | 75,419 | 254,437 | 254.4 | −6% |

for the 3D printed prototype, they represent a feasible option for future manufacturing through additive manufacturing and casting process, if needed. Fig. 2 displays the 3D geometry of all the new fins designed for this study.

## 3. Numerical simulation setup and validation

### 3.1. Physical and mathematical model

The initial numerical simulations were validated using the experimental findings of El-said et al. [61]. One of the primary motivations behind this research was to minimise computational time and cost on a holistic level. To achieve this, certain methods allow conducting simulations with half designs or geometries, assuming setups exhibit symmetry. However, the current study deals with non-symmetrical shapes and complex geometries, which may result in non-symmetrical flow characteristics. Therefore, the experimental setup was replicated for validation purposes to ensure more reliable and robust findings. Therefore, achieving an optimised number of meshing and nodes was preferred to save on computational time and cost. In the experiments of El-said et al. [61], an extended area of 200 mm exists on either side of the test section; therefore, the inlet effect or outlet reflux is avoided by default. The pressure drop in the system was also relatively minimal due to the extended length of the fluid domain, no flow re-circulation, and the outlet being exposed to atmospheric pressure. Conventionally, Reynolds Number (Re) $< 2000$ tends to be laminar flow; transition region, $2000 < Re < 4000$; turbulent flow is $Re > 4000$ [82]. However, for flows in micro scales, diverse and conflicting characteristics are reported. Extant research reported transition and turbulent flow regions within micro-scale flows for $300 < Re < 2000$ [83]. Therefore, in this paper, flows with $Re > 3000$ were assumed as turbulent. Consequently, a standard $\kappa - \epsilon$ model was chosen for turbulence modelling. The simulations were performed with single-phase phenomena considerations, as the working fluid is air. Additionally, adapting and modifying previous research [6,68,84–87], the simulations considered the following assumptions:

1) The working fluid (air) is incompressible;

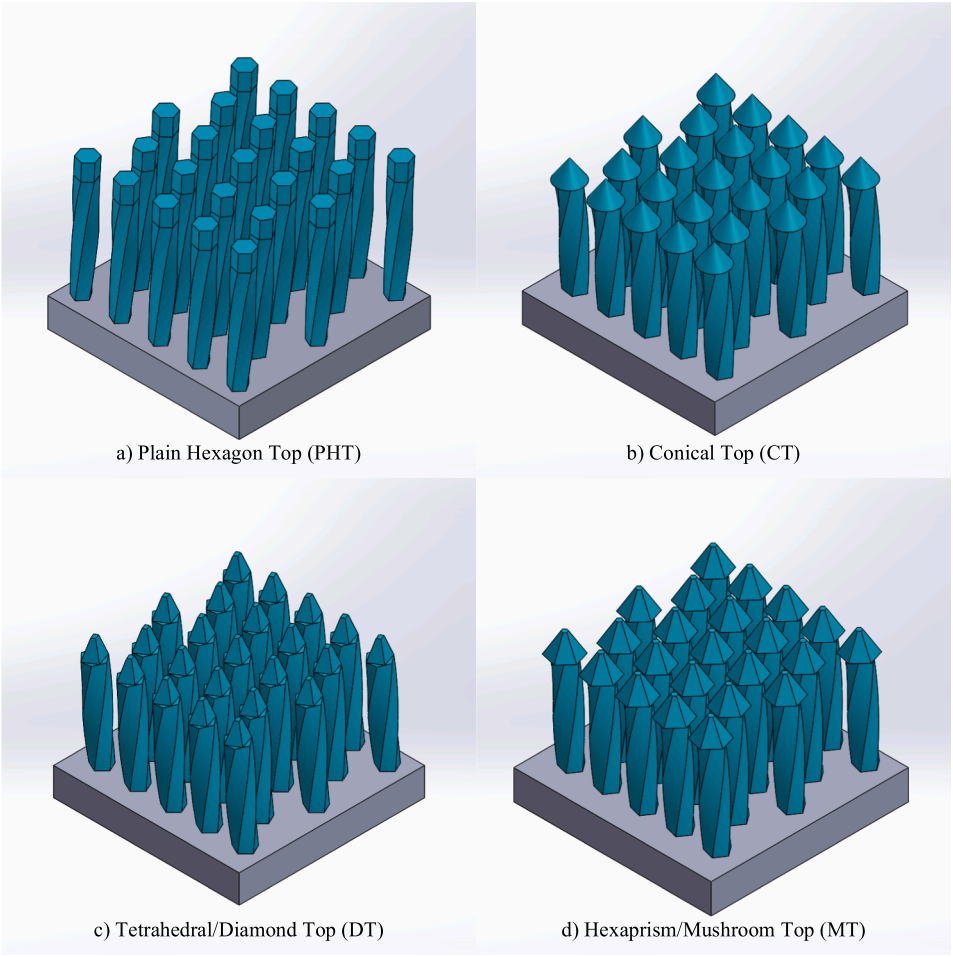


**Fig. 2.** All biomorphic scutoid pin–fin designs: a) Plain Hexagon Top (PHT), b) Conical Top (CT), c) Diamond Top (DT), d) Mushroom Top (MT).

2) Gravity can be ignored due to the low mass of air;
3) The material properties are isotropic;
4) Surface radiation and viscous heat dissipation are negligible.

The baseline governing equations for simulations, validation, and data reduction were:

Continuity equation:

$$\frac{\partial U}{\partial X}+\frac{\partial V}{\partial Y}+\frac{\partial W}{\partial Z}=0 \tag{1}$$

Energy equations:

$$\rho_f\left(u\frac{\partial T}{\partial x}+v\frac{\partial T}{\partial y}+w\frac{\partial T}{\partial z}\right)=\mu\bullet\Pr\left(\frac{\partial^2 T}{\partial x^2}+\frac{\partial^2 T}{\partial y^2}+\frac{\partial^2 T}{\partial z^2}\right)+S_t(fluid) \tag{2}$$

$$k_s\left(\frac{\partial^2 T_s}{\partial u^2}+\frac{\partial^2 T_s}{\partial y^2}+\frac{\partial^2 T_s}{\partial z}\right)=0(solid) \tag{3}$$

$$\text{Dimensionless parameters}: X=\frac{x}{D_h},\ Y=\frac{y}{D_h},\ Z=\frac{z}{D_h},\ U=\frac{u}{u_{in}},\ V=\frac{v}{u_{in}},\ W=\frac{w}{u_{in}}$$

Conductive heat transfer/Fourier's law

$$Q=-kA\frac{\partial T}{\partial x} \tag{4}$$

Where, thermal conductivity ($k$) is a thermophysical constant,

$$K=\frac{Qd_p}{A\Delta T}$$

Mean convective heat transfer coefficient (HTC):

$$h=\frac{\dot{m}_a c_{p,a}\left(T_{out,a}-T_{in,a}\right)}{A_s\left[T_b-\left(\frac{T_{in,a}+T_{out,a}}{2}\right)\right]} \tag{5}$$

Nusselt Number ($Nu$):

$$Nu=\frac{hL_b}{k_a} \tag{6}$$

Thermal Resistance ($R_{th}$):

$$R_{th}=\frac{T_b-T_{a,in}}{\dot{m}_a c_{p,a}(T_{out,a}-T_{in,a})} \tag{7}$$

Fin efficiency ($\eta_F$):

$$\eta_f=\frac{\tanh(\mathrm{M}\times\mathrm{H}_a)}{M\times H_a} \tag{8}$$

$$Where, M=\sqrt{(\frac{4h}{k_f D_h})}$$

Pressure drops ($\Delta P$):

$$\Delta P=(P_{inlet}-P_{outlet}) \tag{9}$$

Performance Improvement Factor (PIF):

$$PIF=\left(\frac{h_{(nc)}}{h_{(bc)}}\right)/\left(\frac{\eta_{f(nc)}}{\eta_{f(bc)}}\right)^{\frac{1}{3}} \tag{10}$$

### 3.2. Grid independence and numerical validation

ANSYS Fluent's Finite Volume Method (FVM) was used for simulations and meshing. A mixture of hybrid and rectangular-grid type meshing was implemented to increase the overall mesh quality whilst reducing computational time and meshing nodes. The mesh independence test was conducted and compared with the experimental data for rectangular pin-fins for validation of the simulation setup; this was the base design (SPF). The element sizes of the solid domain were 0.004 mm, 0.0035 mm, and 0.003 mm; the element size of the fluid domain varied from 0.002 to 0.001 mm. The three different meshes (with varying element count) were *Mesh I* (164269), *Mesh II* (255186), *Mesh III* (530970), respectively. The element sizes were chosen and adjusted based on a target average orthogonal quality. The average orthogonal quality of the mesh was over 0.75 (very good). Refinement ratios between two different mesh types were above 1.3. The grid validation considered two variables: maximum velocity at the outlet, $V_{max(out)}$, and average temperature of the outlet, $T_{avg(out)}$. The numerical validation considered the heat transfer coefficient, HTC ($h$), from $Re = 3182 to 9971$. The grid independence results are summarised in Fig. 3; it shows that deviations between the corresponding mesh qualities are minimal. Furthermore, to complement the visualisation in Fig. 3 and Fig. 4, Table 2 displays a sample of the mesh and grid independence results, providing a quantitative assessment of the values obtained for accuracy and uncertainty.

After considering all the findings and computational time, Mesh II was taken as the preferred option for simulations. Fig. 4 shows the deviation between the numerical simulations and experimental data [61]. As mentioned earlier, Re < 4000 values are generally in the transitional range before turbulent flow conditions occur. Therefore, using the $\kappa-\epsilon$ model, the initial value overshoots by 10 %, but after that, in higher Re values, the data points are relatively consistent.

### 3.3. Meshing and boundary conditions

One of the objectives of our research was to appraise different volume and implement machine learning. Hence, after the numerical validation, to avoid overfitting of the data and enable a more broader data analysis, the operating conditions were slightly changed to investigate higher Reynolds Numbers not examined in the available literature for similar designs. Therefore, the simulations were set up with the following boundary condition: a uniform velocity and constant temperature at the inlet, with values of $u = u_{in}, v = 0, w = 0, T = T_{in} = 298K$; zero pressure at the outlet, and scalable wall function for the near-wall treatment. The heat flux value was $15500 W/m^2$. The mesh interaction boundary was coupled at the fluid–solid contact surface, while all other surfaces were adiabatic. The momentum and energy equations used second-order upwind schemes, and the velocity–pressure coupling was selected using the SIMPLE algorithm having monitors' residual value set to $10^{-5}$ and $10^{-7}$, respectively. Lastly, hybrid initialisation was chosen for the calculations. Fig. 5 illustrates the simulation setup, including the fluid domain, solid domain (pin-fins), and meshing. The simulation fluid and solid domains are depicted with a sliced plane, revealing 3D mesh blocks to provide a more three-dimensional perspective of the mesh employed — the sliced view utilises the base design SPF. Next to the simulation domains, the meshes for the scutoid pin-fins are also presented, with the PHT design view intentionally rotated to offer an alternative perspective of the mesh within the designs. In certain regions or cases, minor or local face refinements were employed to minimise the number of elements or improve the average orthogonal mesh quality.

## 4. Results

### 4.1. Heat transfer performance

Figs. 6–9 illustrate the performance metrics to evaluate the pin-fins. Firstly, Fig. 6 presents a graph that plots the Heat Transfer Coefficient (HTC) against the Reynolds Number (Re). The HTC is significant in thermal management research as it quantifies heat transfer efficiency between a solid surface and a fluid medium. HTC represents the rate at which heat is convectively transferred from the solid metal surface to the surrounding air — in this case. The results reveal that the plain hexagon

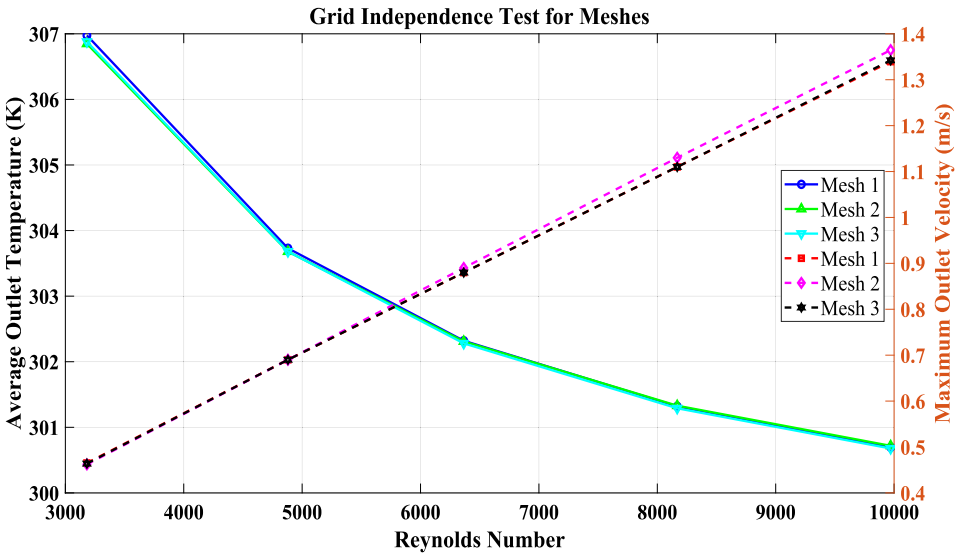


**Fig. 3.** Grid independence test results.

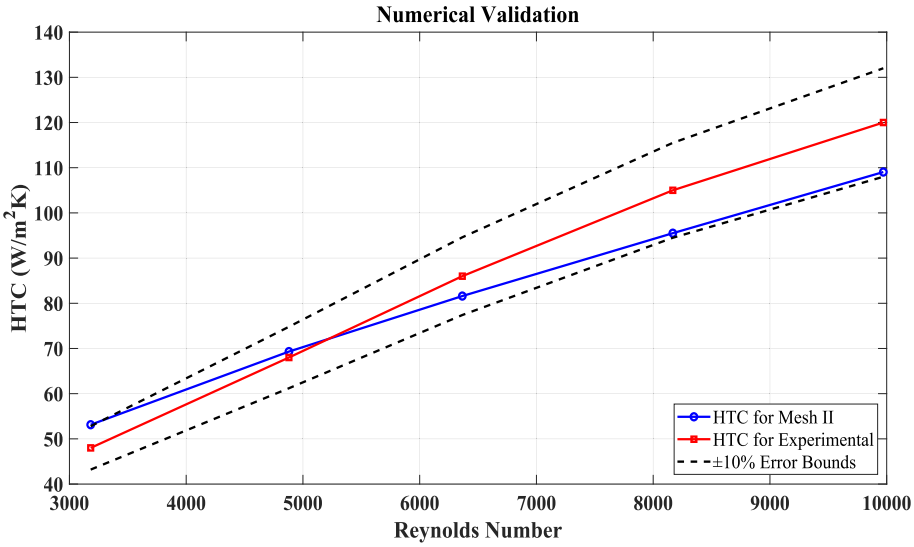


**Fig. 4.** Numerical validation of the simulation.

**Table 2**
Sample grid independence test accuracy results.

| $Re, V_{in}$(3182, 0.3 m/s) | $T_{avg(out)}$(K) | $V_{max(out)}$(m/s) | $h(W/m^2k)$ | %*Deviation*(*h*)[61] |
|---|---|---|---|---|
| Mesh I | 306.98 | 0.47 | 54.96 | 12 % |
| Mesh II | 306.85 | 0.46 | 53.00 | 8 % |
| Mesh III | 306.88 | 0.46 | 56.66 | 16 % |
| $Re, V_{in}$(9971, 0.94 m/s) | $T_{avg(out)}$(K) | $V_{max(out)}$(m/s) | $h(W/m^2k)$ | %*Deviation*(*h*)[61] |
| Mesh I | 300.70 | 1.34 | 107.64 | 12 % |
| Mesh II | 300.72 | 1.36 | 108.48 | 10 % |
| Mesh III | 300.68 | 1.34 | 111.93 | 8 % |

top (PHT), showcases the highest overall HTC, despite having the lowest volume and surface area ($volume(V) = 232541.53\,mm^3$, $surfacearea(SA) = 70646.26\,mm^2$). In comparison, the hexaprism or mushroom-inspired top (MT) design showed, on average, 5 % lower HTC values whilst having the highest material usage among all pin–fin designs ($V = 254437.03mm^3, SA = 75418.77mm^2$). The diamond/tetrahedral top (DT) and conical top (CT) were the two least-performing pin–fin shapes, with CT demonstrating the worst HTC performance ($96.6W/m^2katRe = 5500$). The DT and CT designs might suffer from boundary layer separation or inadequate mixing of the fluid flow. In the case of the conical top (CT) design, its particularly poor HTC performance can be attributed to its geometry, which might induce strong separation of the boundary layer and hinder effective heat transfer.

The Nusselt Number (Nu), similar to the HTC, is a critical metric for assessing heat transfer and provides insights into convective heat transfer properties of systems. By comparing the conductive heat transfer to the convective heat transfer at the surface, the Nu quantifies the convective heat transfer rate. Fig. 7 shows the Nu comparison; since the Nu is directly proportional to the HTC, it exhibits a similar trend. In this study, the plain hexagon top (PHT) design consistently exhibited the highest Nu across different Reynolds Numbers (Re). In contrast, the conical top (CT) design showed the lowest Nu value. The Nu performance of different pin–fin shapes, just like the HTC, can be influenced by flow reversal and recirculation phenomena. Pin-fin shapes that promote flow reversal or recirculation might experience reduced heat transfer rates due to inefficient removal of the heated fluid and replacement with cooler fluid.

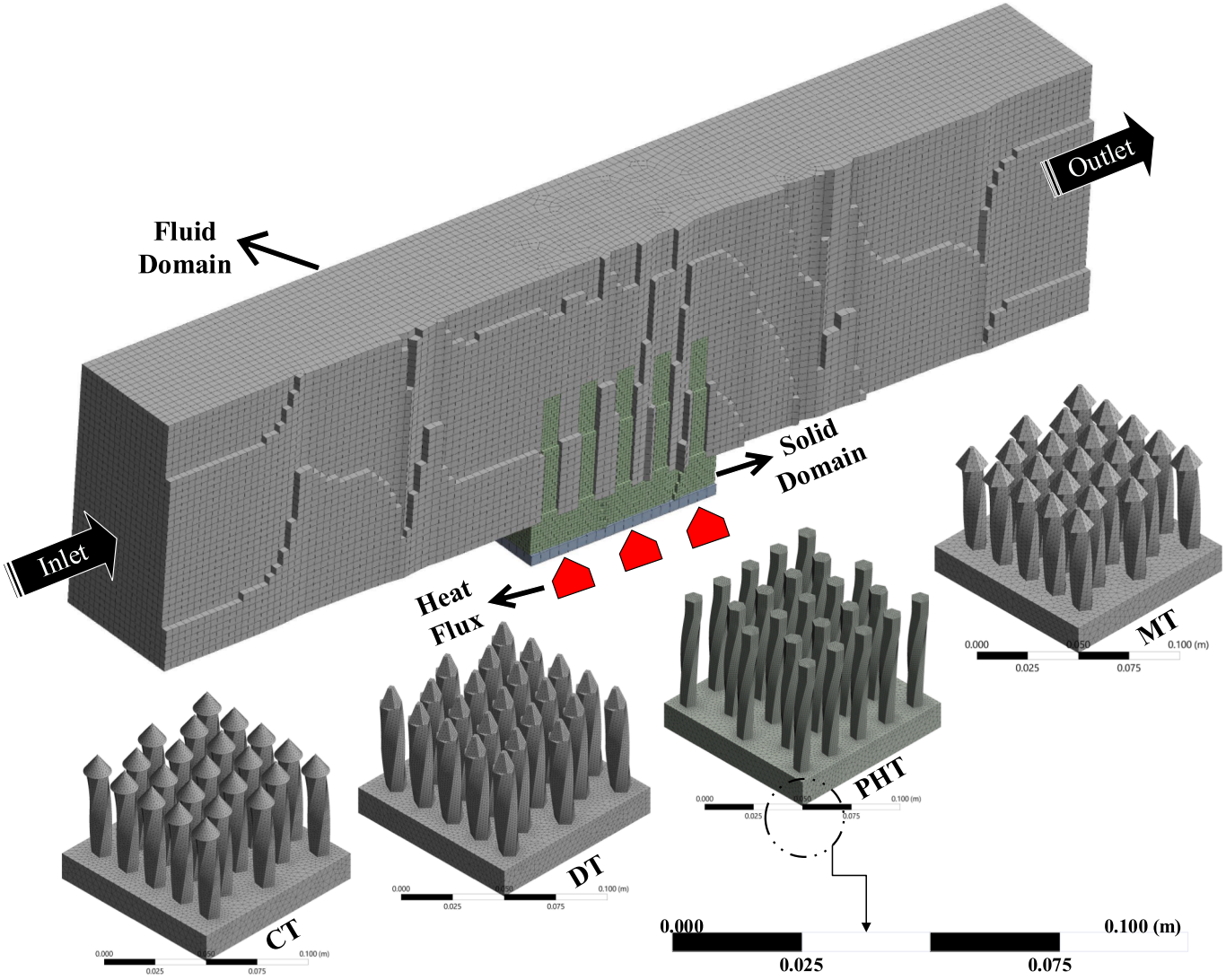


**Fig. 5.** 3D Mesh visualisation of fluid and solid domains for the pin-fins.

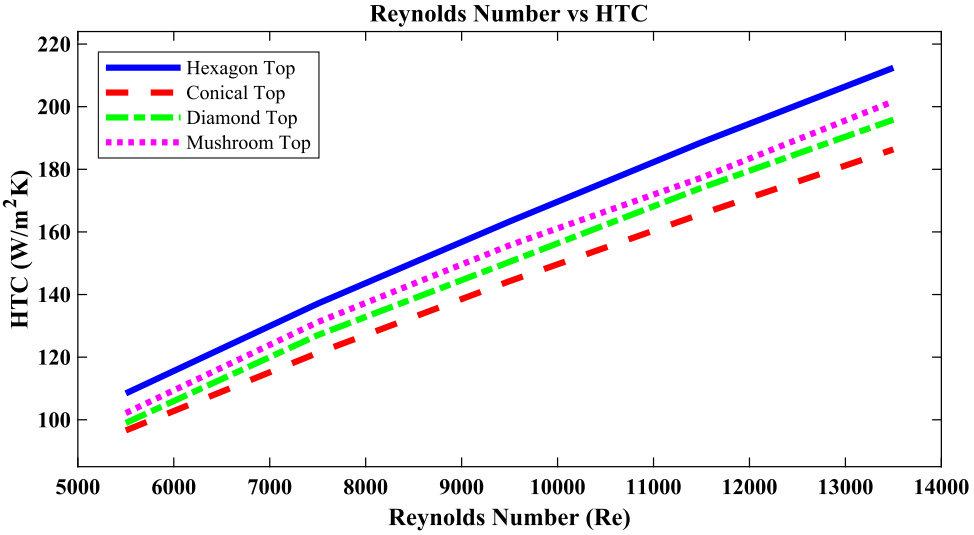


**Fig. 6.** Heat transfer coefficient comparison with different Re.

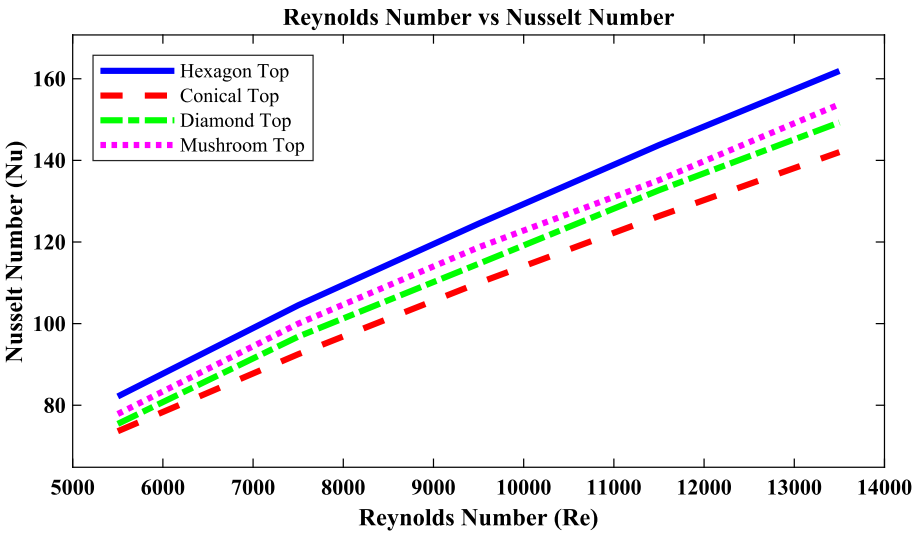


**Fig. 7.** Nusselt Number comparison with different Re.

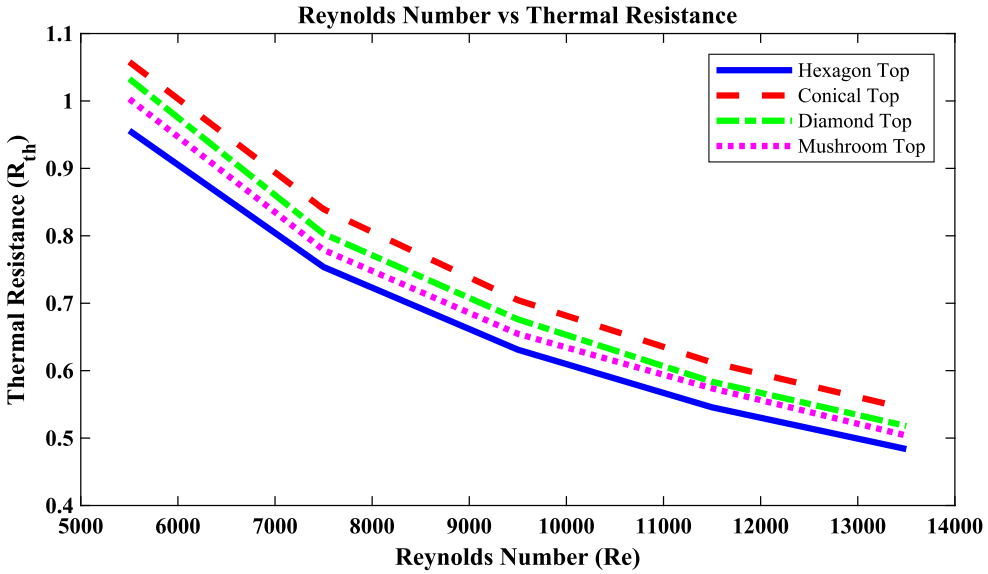


**Fig. 8.** Thermal resistance comparison with different Re.

Fig. 8 illustrates the thermal resistance ($R_{th}$) of the pin-fins. Thermal resistance represents the obstruction to heat flow in a material or system, serving as a fundamental parameter in heat transfer analysis and thermal management. It enables the evaluation and optimisation of the overall thermal performance of heat sinks. Notably, in this case, both the PHT and MT designs, which feature hexagonal bases, exhibited the lowest $R_{th}$ values, indicating their superior heat dissipation capabilities compared to other designs. On the other hand, the DT and CT designs displayed the highest $R_{th}$, with CT demonstrating the most resistance. The thermal resistance of a pin–fin design is influenced by the thickness of the thermal boundary layer surrounding the fins. Designs that effectively reduce the boundary layer thickness can achieve lower thermal resistance. The PHT and MT designs may minimise boundary layer thickness more effectively compared to other designs, leading to lower $R_{th}$ values.

Interestingly, the findings and trends diverged when considering the fin efficiency values depicted in Fig. 9. Fin efficiency ($\eta_F$) is a parameter used to assess the effectiveness of a fin in enhancing heat transfer; it quantifies how efficiently a fin transfers heat from the solid surface to the surrounding fluid medium. Fin efficiency is particularly relevant in heat transfer applications involving extended surfaces or fins, where the primary objective is to increase heat dissipation capacity. Based on the values in Fig. 9, the CT design demonstrated the highest $\eta_f$, followed by the DT, while the MT and PHT designs exhibited the lowest $\eta_f$. However, it is noted that the differences in fin efficiency among the pin–fin designs were minimal ($\leq$1%). Therefore, a marginally lower fin efficiency as a trade-off can be acceptable. The CT design could benefit from smoother flow attachment and detachment along its streamlined shape; this reduces flow separation and enhances the effectiveness of the fin in transferring heat to the surrounding fluid.

### 4.2. Pressure drop and pumping power

In the design and optimisation stage for heat sinks, one of the key considerations includes pressure drop and pumping power expenses [88]. However, as previously mentioned, the reference system exhibited minimal pressure drops mainly due to its open outlet (exposed to atmospheric pressure) and the absence of flow recirculation. Thus, the focus of this study was on enhancing heat transfer and fluid flow

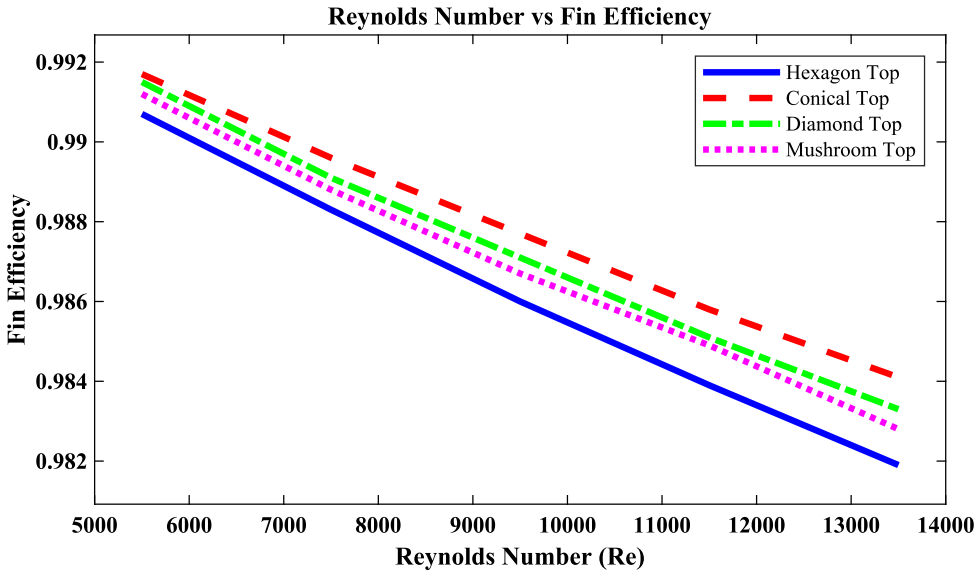


**Fig. 9.** Fin efficiency comparison with different Re.

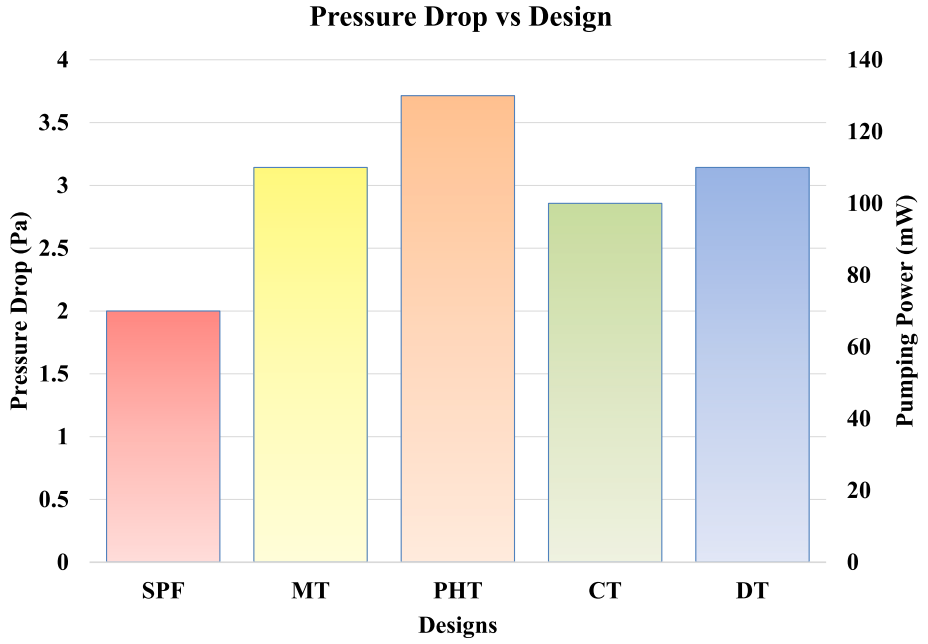


**Fig. 10.** Pressure drop comparisons.

characteristics — with the understanding that any trade-offs in pressure drop would remain within acceptable limits. Fig. 10 shows the pressure drop comparisons. In this investigation, the highest value of Re = 13500 was chosen for comparison for two reasons: i) existing literature lacks experimental/numerical values for similar designs within the Re range of 10,000–15,000; ii) Re = 13500 corresponds to the point of maximum heat transfer in the new designs, implying that it will also lead to the conditions with the highest-pressure drops. Consequently, the highest pressure drop was associated with PHT fins, and the lowest pressure drop was observed in SPF fins. The pressure drop trend is consistent with the heat transfer coefficient (HTC), as PHT had the highest HTC. Furthermore, the simulated pressure drops values closely matched the ranges from previous numerical validations with similar Reynolds Numbers [27,89]. It is important to note that a system's pumping power is directly related to the pressure drop. When comparing the pressure drop values between PHT and SPF, even when factoring in a pump with 70 % efficiency, the resulting increase in pumping power is approximately 55 mW, which remains relatively low. As a result, this trade-off is deemed acceptable in exchange for achieving superior heat transfer rates. Additionally, it can be remarked that the extended flow build-up region length employed in the initial experiment played a role in achieving these low pressure drops and pumping power results.

### 4.3. *Machine learning predictions*

In this study, one of the points of interest was investigating the influence and relationship between the design volume, surface area, and heat transfer in a system. The data indicated that volume manipulation via different geometrical adjustments can help to achieve enhanced heat transfer with material savings. Therefore, this led to the assessment of a prediction model to determine HTC whilst incorporating design properties such as volume and surface area. Accordingly, a combination of

four independent variables (IV) — volume, surface area, Reynolds number (Re), and inlet velocity — was used to predict the dependent variable (DV) — heat transfer coefficient (HTC). The rationale behind this idea was that developing a simplistic model that relates volume to the HTC would have significant implications, as it would provide a quick performance indicator and assessment of heat transfer effectiveness without the need for extensive experiments, CFD simulations, or deep neural networks requiring vast datasets.

Consequently, six different types of machine learning models were compared for predicting the HTC: Multiple Linear Regression (MLR), K-nearest Neighbours (KNN), Random Forest (RF), Gradient Boosting Regression (GBR), and ensemble methods such as Bagging and Stacking. Description and mechanics of all the machine learning models goes beyond the scope of this work and have been extensively detailed in existing literature. While MLR, KNN, and RF have been commonly used [90], GBR and ensemble methods like Bagging and Stacking are relatively unexplored, compared to the popular algorithms such as MLR and RF, especially in heat transfer analysis; thus, these algorithms could produce promising results. GBR employs a boosting technique to create an ensemble of weak predictive models, typically in decision trees [91], while Bagging (also referred to as bootstrap aggregation) and Stacking are ensemble methods that combine multiple models to improve predictions [92]. Regression models generally do not require many data points compared to neural networks; hence, two distinct datasets were created for the machine learning predictions (CFD and Combined). The first dataset consisted solely of data points from CFD — gained from the novel pin-fins produced in this investigation. The second dataset combined CFD simulation and experimental results to form a broader dataset and enhance accuracy or avoid overfitting. The experimental data consisted of rectangular and hexagonal pin-fins' best and worst performing designs from El-said et al. [61]; the volume and surface area information was gained via the SolidWorks evaluation tool. It should be noted that even though the dataset has limited number of points, due to the different types of data considered, it can arguably provide good predictions. Additionally, recent research suggests that condensing datasets and using reduced data can potentially provide better predictions for thermal analysis [93].

The performance of each model was calculated using Root Mean Squared Error (RMSE) and Mean Absolute Percentage Error (MAPE). RMSE measured the average deviation between predicted and actual HTCs, while MAPE assessed the relative errors in percentages. Table 3 shows the data of the model performances. RMSE and MAPE metrics enabled a thorough comparison and ranking of the models' performance. To exhibit the results clearly, a grouped bar graph in Fig. 11 compares the model's predictive capabilities. The evaluation process using RMSE and MAPE ensured an objective assessment of the predictive models and aided in determining the most suitable approach for predicting HTCs in mini channel heat sinks. The results showed that Bagging and Stacking methods had the best performance, with an average MAPE value of 4.6 % and 4.4 % and RMSE values of 8.7 and 8.4, closely followed by MLR at 4.7 % and 8.4. RF and KNN had a poorer performance, with KNN performing the worst among all models. Although GBR had slightly higher errors than the top-performing models, the percentage deviation between the two datasets for GBR was the lowest; this shows that GBR is less sensitive to the differences in datasets. In forced air convection, the HTC values can range between 10 and 500 $(W/m^2k)$ [94]. Therefore, considering the range for prediction, mean MAPE $< 5$ % and RMSE $< 10$ can arguably be considered relatively good and acceptable; this is especially valid considering the original experiments and the CFD simulations had approximately $\pm$ 10 % margin for error.

**Table 3**
Data for machine learning model performance.

| Model Type | RMSE (CFD) | MAPE (CFD) | RMSE (Combined) | MAPE (Combined) |
|---|---|---|---|---|
| MLR | 6.09 | **4.3 %** | 10.72 | 5.0 % |
| GBR | 7.37 | 5.5 % | **9.32** | 4.9 % |
| RF | 6.99 | 4.4 % | 15.71 | 9.0 % |
| KNN | 13.97 | 11.3 % | 15.36 | 7.2 % |
| Bagging | 6.55 | 4.9 % | 10.77 | **4.2 %** |
| Stacking | 6.28 | 4.5 % | 10.56 | **4.3 %** |

### 4.4. Fluid flow characteristics

Fig. 12 (a)–(d) showcases the temperature contours across three planes at Re = 13500 — where the highest heat transfer occurs. The first plane is positioned in the mid-section of the heat sink, the second plane is 0.1 m from the first plane, and the third plane is at the outlet position. Temperature contours provide visualisation of temperature variations across specific regions, enabling interpretation of thermal and flow behaviour.

In Fig. 12a, hotter temperature spots near the bottom portion of the fins are observed, while no apparent similar features are evident at the tops. In the middle/second plane, a thin high-temperature (red colour zone) thermal boundary layer is present; thinner boundary layers can promote better heat transfer performance as seen in Fig. 6. However, the dominant temperature range in the second plane consists of mid-temperature (300 K – 306 K) values. Fig. 12b illustrates the temperature distribution in the CT design. One primary difference between CT and PHT is the presence of localised hotter regions around the conical tops, extending beyond the solely bottom portion that was observed in Fig. 12a; this indicates that the contact between air and the pin-fins are more prominent compared to the other design and validates the initial assumption of better flow attachments leading to higher fin efficiency in Fig. 9. At the outlet, a high-temperature region appears, and it is broader compared to PHT, forming sinusoidal-shaped thermal layers; this denotes the presence of uneven flow distribution.

Fig. 12c depicts the temperature contours for DT. Akin to Fig. 12a, there is no region of high temperature (red zones) at the top of the fins, but the bottom portion exhibits higher temperatures (1 K to 1.2K more) than the surrounding air. Interestingly, a localised cold spot or anomaly is present at the bottom-right position of the outlet, due to uneven flow distribution and inefficient flow mixing; hence, this will be further investigated in the next sections to assess the flow characteristics and turbulence buildup in DT. Lastly, Fig. 12d shows the temperature distribution of the MT fins. The temperature contours of MT are similar to those of CT; however, some notable differences exist. In the middle plane, the temperature regions showed distinct thermal boundary layers, more pronounced than CT; thus, showing a more even flow distribution/less turbulence compared to CT. Nevertheless, the outlet section displays a sinusoidal distribution of thermal boundary layers, similar to CT, but with a slightly lower the maximum outlet temperature — 0.5 K less than CT.

Fig. 13 (a)–(d) depicts the velocity contours at Re = 13,500. Velocity contours are valuable tools for understanding fluid flow patterns and dynamics. They provide visualisation of fluid velocities across specific regions or objects, such as heat sinks. In this study, for a more thorough understanding of heat transfer and fluid flow characteristics, various parameters were evaluated from distinct points of interest across multiple perspectives. Fig. 12 showed temperature contours, emphasising the diverse temperature distribution across three important regions. Meanwhile, the velocity contours concentrated on delineating the velocity and its boundary layers between and behind the pin fins, ultimately guiding the flow toward the outlet. This visualisation of flow features from different viewpoints, using different metrics or parameters, provided a deeper insight into the underlying flow characteristics and physics. The contours were drawn in the exact mid-plane of the heat sinks; as mentioned earlier, due to the minor differences pin–fin spacing and geometry, the pins (white cavities) are not identical.

Fig. 13a illustrates the velocity distribution within the PHT fins region. Notably, PHT exhibited no significant dead (blue) zones alongside

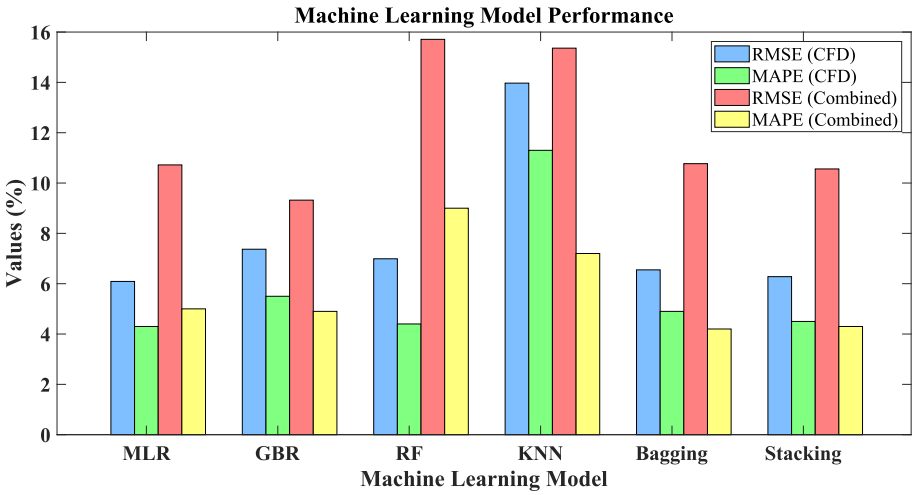


**Fig. 11.** Comparison of machine learning model performance.

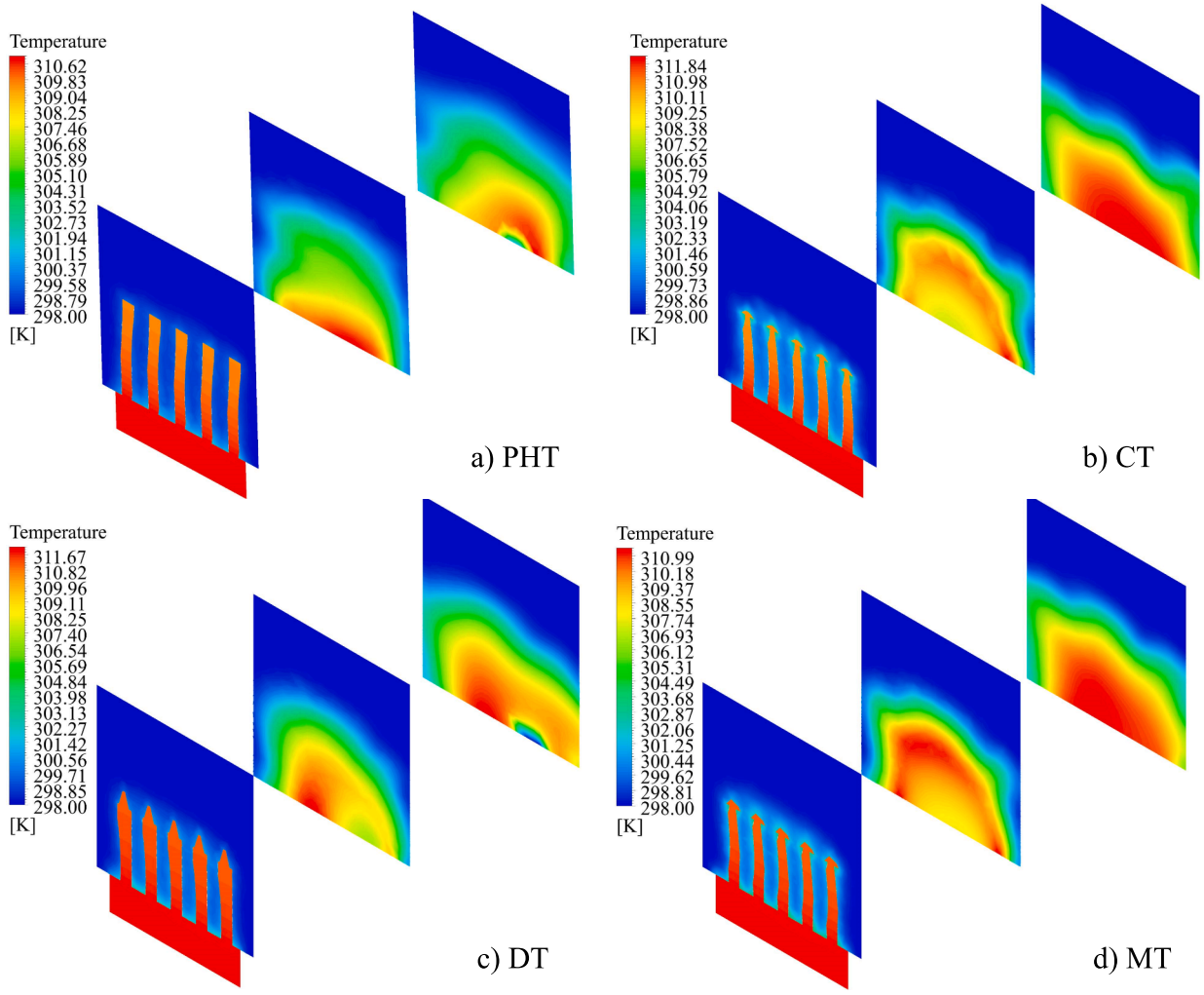


**Fig. 12.** (a)–(d). Temperature contours of all scutoid pin-fins (planar views).

the pin-fins compared to the other designs, where such zones are apparent in distinct points, such as the bottom of the fins (DT) or the last row (CT) in Fig. 13b and c. Concerning the "top" features in Fig. 13b, c, and d, designs with pointed tops like CT, DT, and MT show noticeable flow separation, forming thick boundary layers of rapidly moving air above the pin fins; the varying thick boundary layers ultimately reduce the heat transfer efficiency. The most pronounced velocity hotspot for flow separation was observed on the first row of pin-fins in the CT design (maximum velocity = 2.86 m/s), due to the pointed tops. Additionally, in the PHT design, the boundary layer (red) on top of the fins appears

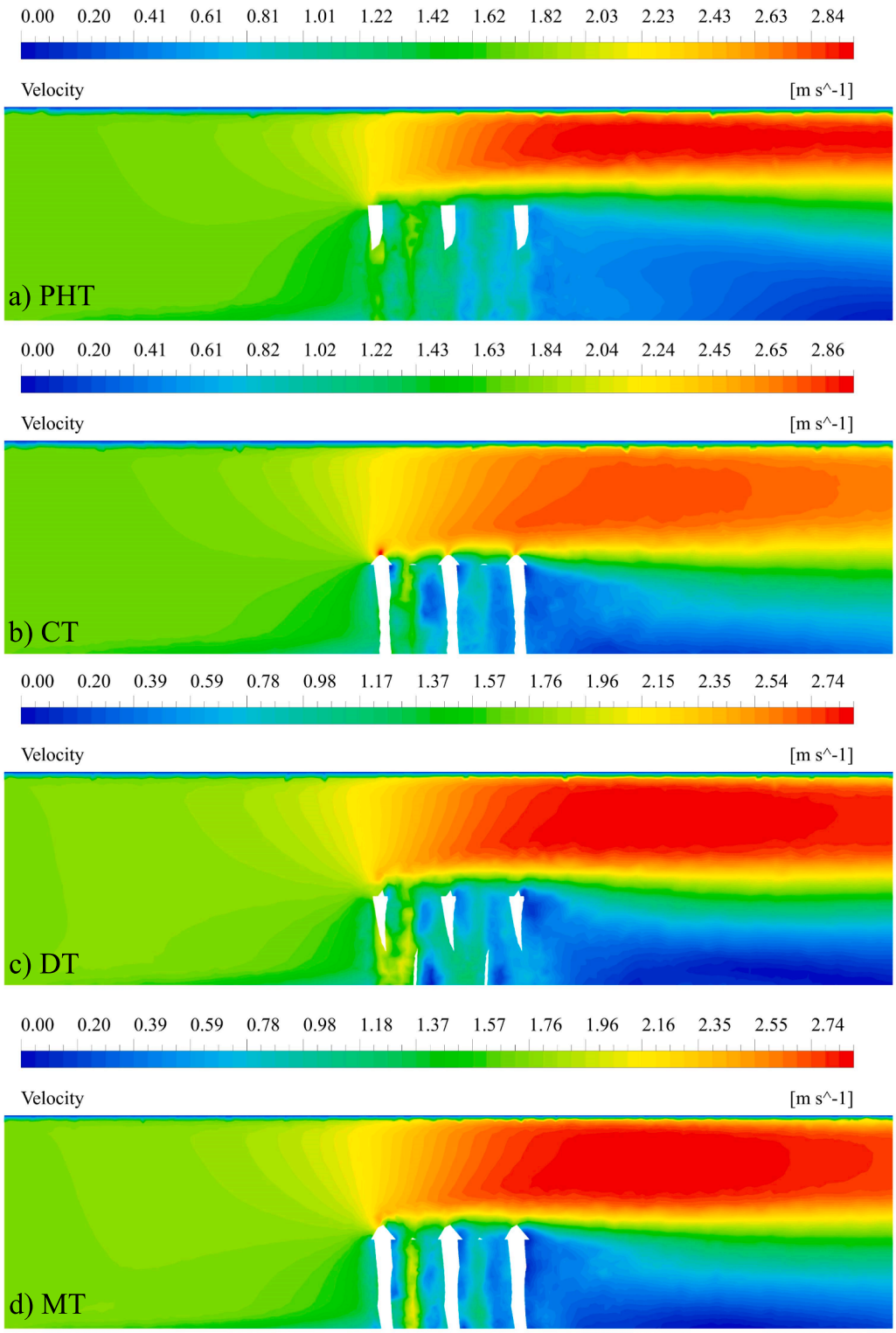


**Fig. 13.** (a)–(d). Velocity contours of all scutoid pin-fins (side view).

comparatively thinner than the other designs; this was primarily due to the 5 % increased height, showcasing positive implications of the height increase. PHT also recorded the second highest maximum velocity among the designs (2.84 m/s), while DT exhibited the lowest (2.74 m/s). Observing the wake profile behind the pin fins in all the designs of Fig. 13(a)–(d), it becomes evident that PHT fins had a steady and widespread wake compared to other designs, hinting at a steady or slow-moving flow. Conversely, other designs displayed a relatively larger gap between fast-moving red regions and slow-moving thick dead regions (dark blue). Therefore, such a difference between fast and slow-moving fluids will lead to high-pressure and low-pressure zones. Although there is a relationship between pressure drop and wake profiles behind objects, the geometrical variations led to an acceptable level of minimal overall system pressure drop as shown in Fig. 10, and the differences in pressure changes within that region were not significant enough (cross-checked using a data probe point and pressure contours, yielding values

less than 1 Pa). As mentioned earlier, such minor pressure differences were expected in these systems. Thus, to better comprehend the differences in flows and turbulence, the next sections focused on streamline velocity and turbulent kinetic energy.

Fig. 14 (a)–(d) displays the Turbulent Kinetic Energy (TKE) contours for the pin-fins at Re = 13500. It can be remarked that TKE parameters are not commonly used in thermal analyses of pin–fin-based heat sinks, primarily due to the complexities associated with turbulent flows. However, TKE patterns can offer crucial insights for comparing the fluid dynamics of a system. TKE involves the conversion of kinetic energy from chaotic eddy motion into thermal energy [95]. Moreover, TKE contours provide valuable insights into the spatial distribution and intensity of turbulence within flows. In Fig. 14, the TKE contours visually represent dissipation patterns and aid in identifying turbulent hotspots, offering a top-down perspective of the designs.

The figures revealed that, in comparison to other designs, Fig. 14a

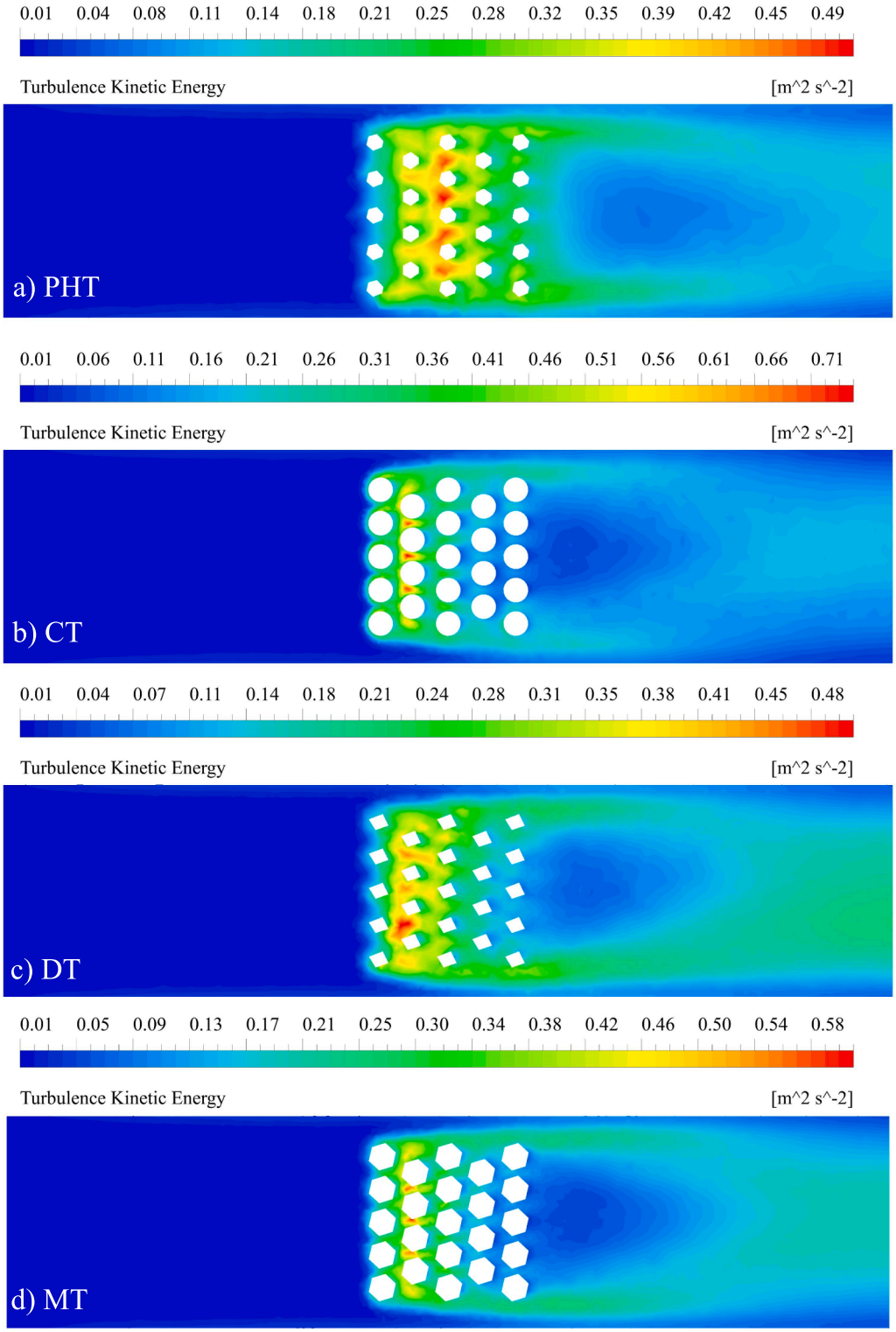


**Fig. 14.** (a)–(d). Turbulent kinetic energy contours of all pin-fins (top view).

showing PHT fins displayed a more evenly distributed TKE within the pin-fins at the centre of the heat sinks. Furthermore, the PHT designs exhibited some turbulence throughout all the fins. While in other designs, TKE intensity diminished after the initial rows of pin-fins, with a wake profile immediately behind the last row; this suggests a transition to laminar flow or turbulence not contributing to thermal energy conversion. In Fig. 14b and d, showing CT and MT, the second row of pins generated the two highest maximum turbulence values (7.13 Joules and 8.84 Joules) due to top features acting as a restrictor between the pin fins, compressing airflow into thinner lanes, promoting faster fluid movement and higher energy conversion and efficient flow mixing. Conversely, PHT featured no such flow restrictors, resulting in less intense and spread-out turbulence wake profiles; thus, it contained reduced maximum TKE (4.89 Joules). In Fig. 14c highlighting DT, a turbulence hotspot, notably in the lower second row of fins, created an asymmetrical wake profile that leans slightly left, potentially contributing to localised hotspots observed in Fig. 12c's temperature contours. Despite CT and MT having the highest turbulence values, turbulence intensity decreased after the third row of fins, evident in small localised blue regions; this indicates flow separation and recirculation. Consequently, evaluating velocity streamlines around the pin-fins and turbulence near the outlet in the following section is crucial for understanding flow development before reaching the outlet.

Fig. 15 (a)–(d) offers insights into the underlying mechanisms by combining velocity streamlines and TKE contours (outlet). Except PHT, all other designs showed flow instability and vortex formations behind the pin-fins. The extended top features caused these flow disturbances and detachments that resulted in flow recirculation, eddy formation, and reversed flow behind the fins, contributing to the dead zones observed in previous figures' contours. The difference between fast and slow-moving fluid layers, combined with pressure differences, played contributing roles in vortex formation. However, the geometry's shape and pin-tops appeared to have a greater influence, as shown in Fig. 15b and 15d depicting CT and DT, respectively. Flow separation leading to localised cold spots in temperature contours was also influenced by vortex formation in DT — depicted in Fig. 15c. Additionally, CT and DT showed the most intense vortices, resulting in the highest turbulent kinetic energy at the outlet, while PHT displayed minimal or no vortex formations due to the lack turbulent flow mixing and the geometry causing efficient flow movement. Active and passive vortex formations have been shown to enhance heat transfer efficiency [96]. However, studying vortex-related heat transfer goes beyond the scope of this work.

## 5. Discussion

The findings from this study on heat transfer and fluid flow provide insights into the performance, underlying mechanisms, and limitations of various pin–fin designs. The combination of CFD, experimental data, and machine learning helps bring a fresh perspective in the development of hybrid bio-inspired pin–fin designs, along with the possible reduction in manufacturing time and costs. Evaluating performance metrics such as heat transfer coefficient (HTC), Nusselt Number (Nu), thermal resistance, fin efficiency, velocity, temperature, and turbulent kinetic energy (TKE) allows for a critical assessment of the heat transfer characteristics

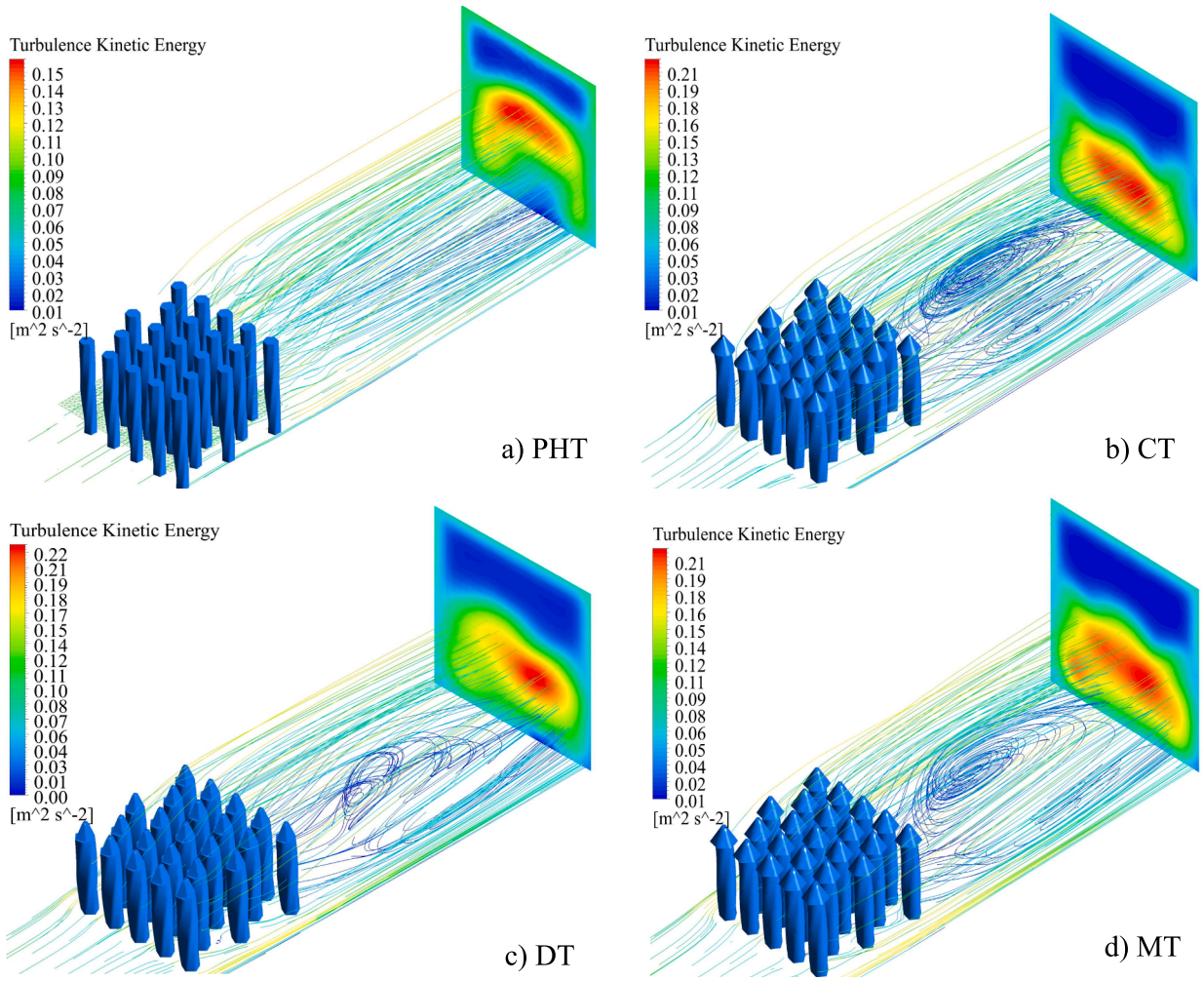


**Fig. 15.** (a)–(d). Combined velocity streamlines with TKE outlet contours (isometric view).

and thermal performance of the novel scutoid-based pin-fins having non-conventional geometry.

The results presented in Figs. 6 and 7 highlight the dominant performance of the plain hexagon top (PHT) design in terms of HTC and Nu. Surprisingly, despite having the lowest volume and surface area, the PHT design consistently demonstrates the highest heat transfer efficiency. For reference, the base geometry (SPF) had a volume of $V = 275000mm^3$, $mass = 275g$. Thus, this raises questions about the prevailing understanding of the correlation between enlarging geometry and heat transfer performance. On the other hand, the Mushroom Top (MT) design, with its larger volume and surface area, exhibits slightly lower HTC values, indicating a potential trade-off between geometric complexity and heat dissipation capability. Fig. 16 presents a comparison of the designs at Re = 13500. By comparing the best-performing PHT design (in terms of HTC) against the worst and second best-performing alternatives, it was observed that PHT had approximately 8.6 % and 7.2 % less mass/volume than MT and CT. Despite its lower mass/volume, PHT demonstrates around 5.2 % and 14 % higher HTC than MT and CT, respectively. Furthermore, with 1.6 % more mass/volume than CT, MT exhibits approximately 8.3 % higher HTC than CT; however, this is to be expected due to the larger surface area.

Based on the graphical values and simulation results, the variation in heat transfer coefficients (HTC) and Nu among the different pin–fin designs can be attributed to different factors. Despite having the lowest volume and surface area, the PHT design exhibits the highest HTC, due to its geometry promoting better fluid flow and heat transfer. Conversely, the hexaprism or mushroom-inspired top (MT) design, with higher material usage and surface area, shows slightly lower HTC values because of flow reattachment and separation around its protruding elements. The least-performing designs, diamond/tetrahedral top (DT) and conical top (CT), suffer from boundary layer separation and inadequate mixing, especially the CT design, which demonstrates the worst performance due to its geometry inducing strong boundary layer separation and intense vortex formations. All these factors interacted to influence heat transfer performance, with turbulence enhancement, flow reversal, and thermal boundary layer thickness also playing roles in determining the HTC of each pin–fin design. The underperformance of the conical top (CT) and diamond/tetrahedral Top (DT) designs in HTC and Nu further emphasises the need for critical evaluation of the assumptions and design principles underlying conventional and non-conventional pin–fin configurations. This is because a shape which had positive impacts previously may negatively affect heat transfer based on modifications, as shown in this study.

With increasing Re, the thermal resistance ($R_{th}$) decreases due to the increased velocity. Examining the thermal resistance results presented in Fig. 8, it is evident that the PHT and MT designs, featuring hexagonal bases for their top features, outperform other designs relating to thermal resistance. Comparing range of $R_{th}$, PHT had 7.2 % and 7.4 % lower range than CT and DT; similarly, MT had 2.9 % and 3.1 % lower range of $R_{th}$ than CT and DT. This potentially suggests that the pin–fin tops' base shape and the resulting flow characteristics play a crucial role in determining the overall thermal performance of the heat sinks. The variation in thermal resistance among the different pin–fin designs can be attributed to several physical factors related to heat transfer and fluid dynamics. Notably, the PHT and MT designs, both featuring hexagonal top features, promotes better heat transfer, minimised boundary layer thickness, efficient heat conduction paths, and adequate flow mixing. Conversely, the diamond/tetrahedral top (DT) and conical top (CT) designs suffer from boundary layer separation and lower heat transfer rates due to their geometrical features. These findings underscore the importance of optimising pin–fin designs to minimise thermal resistance for improved thermal management efficiency. Therefore, the higher thermal resistance observed in the CT and DT designs, particularly in the CT design, raises concerns about their suitability for high-performance heat dissipation applications.

The assessment of fin efficiency in Fig. 9 reveals slightly different trends among the pin–fin designs. While the CT design demonstrates the highest fin efficiency, the differences among the designs are minimal; thus, a potential trade-off can be considered if other heat transfer parameters give superior results. The surface shape/roughness, from edges or sharp features, of the fin structures can influence turbulence levels in the fluid flow, affecting heat transfer efficiency. The specific configurations of the CT and DT designs promote turbulence enhancement, contributing to their higher fin efficiency values; nevertheless, the sharp hexagonal tops promote better overall heat transfer. Therefore, adding chamfers or smooth edges can strike a balance within these designs. The marginal differences in fin efficiency underscore the need to explore alternative design approaches that prioritise overall thermal performance and heat dissipation capability over specific geometric characteristics. The minimal pressure drops and pumping power is another metric where the trade-off can be arguably deemed acceptable for this case due to the superior heat transfer performance of the hexagon-top-based designs.

To further understand the heat performance enhancements of the new pin-fins alongside their trade-offs, the Performance Improvement Factor (PIF) was compared between the new design and the base design. The PIF calculations revealed that, compared to the base design, the heat transfer performance was improved by 1.70, 1.50, 1.56, and 1.60 times using the designs PHT, CT, DT, and MT, respectively. Moreover, this investigation presented a variety of parameters for comparison. Therefore, Fig. 17 consolidates and synthesises the findings of this research to highlight which designs exhibit the best performance. However, due to the significant differences in parameter ranges and their units (e.g., Rth values are 200 times smaller than HTC values), the heatmap/colormap

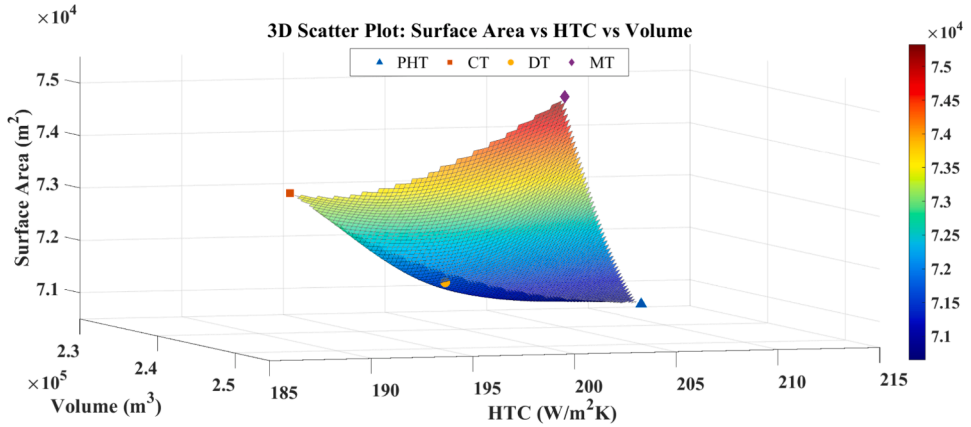


**Fig. 16.** Mass, volume, and heat transfer performance comparison at Re = 13,500.

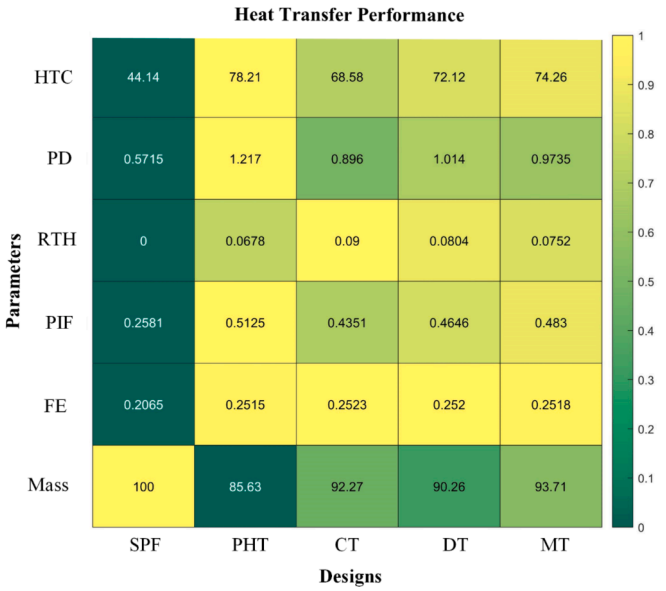


**Fig. 17.** Colormap and summary of heat transfer performance of all design.

was generated using normalised and scaled data, often used in machine learning-related data analysis, to make it dimensionless [97]. Linear scaling of the original data was employed to convert it into values ranging between 0 and 100, where dark green indicates minimum values and yellow indicates maximum values (as shown by the colourmap legend). The heatmap visualisation offers a mixed-method (qualitative and quantitative) approach to gain a condensed understanding of heat transfer performance improvements and comparisons between the base and new designs within this study. The best-performing designs can be inferred using either colour alone or both colour and data. The heatmap, illustrating six parameters [Heat Transfer Coefficient (HTC), Pressure Drop (PD), Thermal Resistance (RTH), Performance Improvement Factor (PIF), Fin Efficiency (FE), and Mass], consistently demonstrates that PHT and MT designs are the overall optimal designs and outperform the conventional designs and geometries.

The assessment of velocity and temperature contours, along with TKE and velocity streamlines, offered insights into fluid flow behaviour, temperature distributions, and energy dissipation within pin–fin structures. The PHT design exhibited relatively even velocity distribution and efficient heat dissipation, while the CT design shows concerns regarding flow separation and turbulence hotspots. In contrast, the DT design presented challenges in achieving efficient heat transfer due to the asymmetrical wakes and presence of cold spots. The presence of hotspots and variations in TKE across designs underscore the complexity of turbulent flows and highlight the need for comprehensive analysis for heat transfer effectiveness throughout the fin structure. As one of the primary objectives of this study was to investigate the underlying physical mechanisms in air-cooled heat transfer strategies, several key insights were observed:

1) Utilising complex fin geometries manufactured through additive manufacturing can enhance heat performance while reducing weight. The data and numerical simulations verified the initial assumptions that these intricate geometries can effectively disrupt airflow without inducing significant flow instability and offer improved heat dissipation, demonstrating the potential for improved heat transfer beyond the traditional surface area relationship;
2) The incorporation of twisted scutoid geometry and various hybrid pin–fin topologies can augment heat transfer by manipulating boundary formation above the pin-fins and controlling wake region formation between and behind the fins. However, careful monitoring of pin–fin spacing, and height is crucial for optimal heat transfer performance within acceptable trade-off limits. Greater pin–fin height can promote thinner boundary layers and uniform flow distribution;
3) Sharp-edged top designs tend to outperform pointed or curved surfaces. While pointed or conical surfaces may induce flow separations, they result in the formation of intense passive vortices and increased wake or dead zones. Further investigation into passive vortex manipulation is warranted in air-cooled heat sinks to refine heat transfer strategies;
4) Pin-fin geometry not only influences heat transfer but also impacts thermal resistance and pressure drop within the system, particularly under varying operating conditions. Previous studies showed that conical and tetrahedral geometries have promising results, yet their effects on temperature distribution along the fins and behind the pins can be significant, influenced by factors such as velocity boundary layers and turbulent kinetic energy, leading to non-uniform and unstable flow patterns. All these factors combined ultimately reduced their heat transfer capabilities.

Moreover, moving on to the machine learning model predictions, determining whether volume and surface area could predict the HTC while employing underutilised algorithms such as Gradient Boosting Regressor and ensemble methods in heat transfer analysis, holds several key motivations and advantages. The HTC is a critical factor in determining the efficiency of heat transfer processes. Thus, through understanding the relationship between volume, surface area, and HTC, heat sink designs and other thermal management systems can be optimised. Also, current prediction models can be further utilised via transfer learning methods to help researchers, engineers, and designers develop more efficient and effective cooling solutions, leading to improved performance and energy savings. The current dataset can also be augmented with more experimental and numerical simulations in the future via an open-source database. Additionally, by predicting the HTC based on volume and surface area, the need for extensive and costly experimental testing can be avoided in the design development stage. Instead, these easily measurable geometric parameters can estimate the HTC, significantly reducing both time and resource requirements during the design and evaluation phases. In this era of Industry 4.0, with a continuous reduction in product development times [98], finding innovative solutions via technology is warranted to trigger continuous improvement.

Furthermore, if design properties such as volume and readily available heat transfer parameters prove to be effective predictors of the HTC, as highlighted by the findings of this investigation, it simplifies the modelling process. Instead of relying on complex and computationally expensive simulations, a simpler model could make dependable predictions using available geometric parameters or operating conditions. This simplicity can streamline the design process and facilitate agile analysis of different heat sink configurations. Additionally, this allows flexibility and scalability as the knowledge and predictions can be applied to various applications, providing valuable insights for different engineering scenarios. Moreover, the relationship between volume, surface area, and the HTC contributes to a deeper understanding of the underlying physics and mechanisms involved in heat transfer processes. It enables the study of complex shapes, and new configurations of pin–fin heat sink via additive manufacturing methods, and it allows researchers and engineers to gain insights into how these geometric parameters impact the convective heat transfer characteristics, enhancing their comprehensive knowledge base.

Comparing new designs and setups with multiple existing literature findings can often pose challenges due to differences in operating conditions, characteristic dimensions, and design applications. Furthermore, in some instances, authors may withhold critical data from simulations or experiments due to confidentiality concerns. This research reveals that the hybrid pin-fins with top geometries can outperform traditional shapes and conventional designs in terms of HTC

performance, as reported in prior related studies [61,89]. However, it's crucial to recognise that, depending on the acceptable trade-offs in the application and HTC, our design may or may not also excel or underperform at extremely high Reynolds numbers employed in other investigations. Hence, the availability of future rapid performance indicators, facilitated by machine learning and based on readily available parameters such as volume or surface area, will aid both the design and optimisation stages of heat transfer research and beyond.

Moving forward, the critical findings from this study call for a paradigm shift in pin–fin heat sink design. The traditional reliance on simplistic geometric configurations may limit the potential for optimal heat dissipation. Instead, a holistic approach that considers the intricate balance between flow dynamics, heat transfer efficiency, and energy dissipation patterns should be pursued, especially given the availability of advanced manufacturing techniques. Similarly, advanced techniques and combined approaches involving machine learning, multi-objective optimisation algorithms [99], CFD simulations, and experimental investigations can drive the next generation of heat sinks and enable a broader design choice to identify novel configurations that offer enhanced thermal performance. Furthermore, future research should focus on integrating advanced materials and surface enhancements into complex pin–fin designs to amplify cooling and heat transfer, but with reduced cost [100]. Integrating combined innovative approaches, such as surface coatings, micro/nanostructured surfaces, and additive manufacturing techniques, have the potential to significantly alter flow characteristics and enhance convective heat transfer, thereby overcoming the limitations of conventional designs.

The discussion of the findings emphasises the need for a comprehensive re-evaluation of pin–fin heat sink designs. The dominant performance of the biomorphic PHT and MT design in most metrics, coupled with the limitations observed in other designs, highlights the potential for significant improvements. By embracing a multidisciplinary approach that combines insights from fluid dynamics, heat transfer, machine learning, and design for manufacturing considerations, researchers can unlock the full potential of pin-fins and develop next-generation heat sink solutions with superior thermal performance, reduced size and cost, and improved energy efficiency. Nonetheless, despite ensuring different measures and robust methods to ensure the reliability of this study, it is also important to acknowledge the limitations of this study. The findings rely on a specific set of experimental and simulation conditions and limited data points, and therefore, generalisability to other scenarios needs further assessment. Additionally, while advanced materials and additive manufacturing were discussed as potential avenues for improvement, their practical implementation and scalability need to be explored [62,101]. Future research should address these limitations to ensure the practicality and real-world applicability of the proposed design strategies. Therefore, although the study produces valuable findings, the authors accept the limitations or criticism that may arise related to this investigation.

## 6. Conclusion

In conclusion, this study provides valuable insights into the performance and limitations of various novel pin–fin designs for heat transfer and fluid flow in mini channels. The combination of computational fluid dynamics (CFD), experiments, and machine learning techniques offers a fresh perspective in the development of hybrid biomorphic pin-fins, with potential reductions in manufacturing time and costs. The key findings include:

- Dominant performance of the plain hexagon top (PHT) design in heat transfer coefficient (HTC) and Nusselt Number (Nu), challenging the conventional understanding of the correlation between surface area and heat transfer. The novel scutoid-based designs produce 1.5 to 1.7 times better heat transfer performance with a 6 % to 14 % weight reduction compared to the base rectangular/square fin design;
- Numerical thermal analysis demonstrates the superiority of hexagon-based designs (PHT and MT) and raises concerns about the suitability of conical (CT) and tetrahedral (DT) designs for high-performance heat dissipation. Fin efficiency shows minimal differences among designs, with the CT design having the highest efficiency.
- Temperature, velocity, and turbulent kinetic energy contours highlight the importance of geometry and even velocity distribution within the pin–fin region for efficient convective heat transfer, with the PHT design excelling in this aspect. The CT and DT designs exhibit flow separation regions, compromising heat dissipation uniformity due to intense vortex formation, leading to uneven heat distribution. Turbulent energy dissipation patterns further emphasise the complexity of heat transfer processes but provide insights into the underlying mechanism;
- Machine learning predictions demonstrate the potential of using volume and surface area as predictors of the HTC, simplifying design optimisation and exploration, and providing quick performance indicators. Ensemble methods and multiple linear regression perform the best among the compared models (mean absolute percentage error $<5$ %).

In summary, this study contributes to the knowledge of pin–fin heat sink designs, highlighting the dominance of non-conventional designs and the importance of combining multiple strategies. Integrating advanced design and manufacturing techniques and utilising machine learning can unlock the full potential of pin-fins, leading to next-generation heat sink solutions with superior performance, reduced size, cost, product development times, and improved energy efficiency.

## CRediT authorship contribution statement

**Mohammad Harris:** Writing – review & editing, Writing – original draft, Visualization, Validation, Software, Project administration, Methodology, Investigation, Funding acquisition, Formal analysis, Data curation, Conceptualization. **Hongwei Wu:** Funding acquisition, Formal analysis, Conceptualization, Resources, Supervision, Writing – review & editing. **Anastasia Angelopoulou:** Formal analysis, Supervision, Visualization, Writing – review & editing. **Wenbin Zhang:** Supervision, Visualization, Writing – review & editing. **Zhuohuan Hu:** Project administration, Resources, Supervision. **Yongqi Xie:** Project administration, Resources, Supervision.

## Declaration of competing interest

The authors declare that they have no known competing financial interests or personal relationships that could have appeared to influence the work reported in this paper.

## Data availability

Data will be made available on request.

## Acknowledgement

The authors would like to acknowledge the financial support from the Engineering and Physical Science Research Council (EPSRC), UK (Grant No. EP/X038319/1). This support was provided within the framework of the Horizon Europe project Marie Skłodowska-Curie Actions (MSCA), with Grant No. 101082394. The authors would also like to thank the technical guidance received from Michael Wilkins and Hamza Babar from the University of Hertfordshire. Artificial intelligence related tools have been used for checking grammar and readability purposes.

## References


[1] M. Ahmadian-Elmi, A. Mashayekhi, S.S. Nourazar, K. Vafai, A comprehensive study on parametric optimization of the pin-fin heat sink to improve its thermal and hydraulic characteristics, Int. J. Heat Mass Transf. 180 (2021) 121797, https://doi.org/10.1016/j.ijheatmasstransfer.2021.121797.

[2] M. Mohammadilooey, B. Parizad Benam, A. Ateş, V. Yagcı, M. Çaglar Malyemez, M. Parlak, A. Sadaghiani, A. Koşar, Multiple hot spot cooling with flow boiling of HFE-7000 in a multichannel pin fin heat sink, Appl. Therm. Eng. (2024) 123077, https://doi.org/10.1016/j.applthermaleng.2024.123077.

[3] M.W. Alam, S. Bhattacharyya, B. Souayeh, K. Dey, F. Hammami, M. Rahimi-Gorji, R. Biswas, CPU heat sink cooling by triangular shape micro-pin-fin: Numerical study, Int. Commun. Heat Mass Transfer 112 (2020) 104455, https://doi.org/10.1016/j.icheatmasstransfer.2019.104455.

[4] K. Nilpueng, M. Mesgarpour, L.G. Asirvatham, A.S. Dalkılıç, H.S. Ahn, O. Mahian, S. Wongwises, Effect of pin fin configuration on thermal performance of plate pin fin heat sinks, Case Stud. Therm. Eng. 27 (2021) 101269, https://doi.org/10.1016/j.csite.2021.101269.

[5] J. Jaseliūnaitė, M. Šeporaitis, Performance optimisation of microchannel pin-fins using 2D CFD, Appl. Therm. Eng. 206 (2022) 118040, https://doi.org/10.1016/j.applthermaleng.2022.118040.

[6] R. Singupuram, T. Alam, M.A. Ali, S. Shaik, N.K. Gupta, N. Akkurt, M. Kumar, S. M. Eldin, D. Dobrotă, Numerical analysis of heat transfer and fluid flow in microchannel heat sinks for thermal management, Case Stud. Therm. Eng. 45 (2023) 102964, https://doi.org/10.1016/j.csite.2023.102964.

[7] D. Kesavan, R. Senthil Kumar, P. Marimuthu, Heat transfer performance of air-cooled pin–fin heatsinks: a review, J. Therm. Anal. Calorim. 148 (2023) 623–649, https://doi.org/10.1007/s10973-022-11691-z.

[8] M. Harris, H. Wu, W. Zhang, A. Angelopoulou, Overview of recent trends in microchannels for heat transfer and thermal management applications, Chemical Engineering and Processing - Process Intensification 181 (2022) 109155, https://doi.org/10.1016/j.cep.2022.109155.

[9] D. Panda, S. Dilip Saraf, K.M. Gangawane, Expanded graphite nanoparticles-based eutectic phase change materials for enhancement of thermal efficiency of pin–fin heat sink arrangement, Therm. Sci. Eng. Prog. 48 (2024) 102417, https://doi.org/10.1016/j.tsep.2024.102417.

[10] F. Hadi, H.M. Ali, Z. Khattak, M.M. Janjua, An evaluation of heat transfer and pressure drop performance of superhydrophobic surfaced integral mini-channel heat sinks with nanofluids, J. Therm. Anal. Calorim. 149 (2024) 1515–1533, https://doi.org/10.1007/s10973-023-12735-8.

[11] V. Safari, B. Kamkari, N. Hewitt, K. Hooman, Experimental comparative study on thermal performance of latent heat storage tanks with pin, perforated, and rectangular fins at different orientations, Therm. Sci. Eng. Prog. 48 (2024) 102401, https://doi.org/10.1016/j.tsep.2024.102401.

[12] A. Ateş, V. Yağcı, M.Ç. Malyemez, M. Parlak, A. Sadaghiani, A. Koşar, Flow dynamics characteristics of flow boiling in minichannels with distributed pin fin structures, Int. J. Therm. Sci. 199 (2024) 108912, https://doi.org/10.1016/j.ijthermalsci.2024.108912.

[13] A. Shahsavar, H. Ghazizade-Ahsaee, I.B. Askari, M.M. Rashidi, The numerical analysis in heat transfer, fluid flow, and irreversibility of a pin-fin heatsink under the ultrasonic vibration with different transducer power assignment scenarios, Therm. Sci. Eng. Prog. 49 (2024) 102480, https://doi.org/10.1016/j.tsep.2024.102480.

[14] A. Alkhazaleh, F. Alnaimat, B. Mathew, Characterization of MEMS heat sinks having straight microchannels integrating square pin-fins for liquid cooling of microelectronic chips, Therm. Sci. Eng. Prog. 45 (2023) 102154, https://doi.org/10.1016/j.tsep.2023.102154.

[15] T. İzci, M. Koz, A. Koşar, The effect of micro pin-fin shape on thermal and hydraulic performance of micro pin-fin heat sinks, Heat Transfer Eng. 36 (2015) 1447–1457, https://doi.org/10.1080/01457632.2015.1010921.

[16] S.E. Razavi, B. Osanloo, R. Sajedi, Application of splitter plate on the modification of hydro-thermal behavior of PPFHS, Appl. Therm. Eng. 80 (2015) 97–108, https://doi.org/10.1016/j.applthermaleng.2015.01.046.

[17] R. Sajedi, B. Osanloo, F. Talati, M. Taghilou, Splitter plate application on the circular and square pin fin heat sinks, Microelectron. Reliab. 62 (2016) 91–101, https://doi.org/10.1016/j.microrel.2016.03.026.

[18] V. Yadav, K. Baghel, R. Kumar, S.T. Kadam, Numerical investigation of heat transfer in extended surface microchannels, Int. J. Heat Mass Transf. 93 (2016) 612–622, https://doi.org/10.1016/j.ijheatmasstransfer.2015.10.023.

[19] J. Xie, H. Yan, B. Sundén, G. Xie, The influences of sidewall proximity on flow and thermal performance of a microchannel with large-row pin-fins, Int. J. Therm. Sci. 140 (2019) 8–19, https://doi.org/10.1016/j.ijthermalsci.2019.02.031.

[20] Y. Wang, K. Zhu, Z. Cui, J. Wei, Effects of the location of the inlet and outlet on heat transfer performance in pin fin CPU heat sink, Appl. Therm. Eng. 151 (2019) 506–513, https://doi.org/10.1016/j.applthermaleng.2019.02.030.

[21] V. Saravanan, D. Hithaish, C.K. Umesh, K. Seetharamu, Numerical investigation of thermo-hydrodynamic performance of triangular pin fin heat sink using nano-fluids, Therm. Sci. Eng. Prog. 21 (2021) 100768, https://doi.org/10.1016/j.tsep.2020.100768.

[22] D. Hithaish, V. Saravanan, C.K. Umesh, K.N. Seetharamu, Thermal management of Electronics: Numerical investigation of triangular finned heat sink, Therm. Sci. Eng. Prog. 30 (2022) 101246, https://doi.org/10.1016/j.tsep.2022.101246.

[23] J. Zhao, S. Huang, L. Gong, Z. Huang, Numerical study and optimizing on micro square pin-fin heat sink for electronic cooling, Appl. Therm. Eng. 93 (2016) 1347–1359, https://doi.org/10.1016/j.applthermaleng.2015.08.105.

[24] A. Khalili Sadaghiani, A. Koşar, Numerical investigations on the effect of fin shape and surface roughness on hydrothermal characteristics of slip flows in microchannels with pin fins, Int. J. Therm. Sci. 124 (2018) 375–386, https://doi.org/10.1016/j.ijthermalsci.2017.10.037.

[25] Y. Jia, G. Xia, Y. Li, D. Ma, B. Cai, Heat transfer and fluid flow characteristics of combined microchannel with cone-shaped micro pin fins, Int. Commun. Heat Mass Transfer 92 (2018) 78–89, https://doi.org/10.1016/j.icheatmasstransfer.2017.11.004.

[26] S. Souida, D. Sahel, H. Ameur, A. Yousfi, Numerical simulation of heat transfer behaviors in conical pin fins heat sinks, Acta Mechanica Slovaca 26 (2022) 32–41.

[27] D. Sahel, L. Bellahcene, A. Yousfi, A. Subasi, Numerical investigation and optimization of a heat sink having hemispherical pin fins, Int. Commun. Heat Mass Transfer 122 (2021) 105133, https://doi.org/10.1016/j.icheatmasstransfer.2021.105133.

[28] P. Li, Y. Luo, D. Zhang, Y. Xie, Flow and heat transfer characteristics and optimization study on the water-cooled microchannel heat sinks with dimple and pin-fin, Int. J. Heat Mass Transf. 119 (2018) 152–162, https://doi.org/10.1016/j.ijheatmasstransfer.2017.11.112.

[29] A.O. Elsayed, Numerical investigation of heat transfer from multi-bulges pins,, Case Stud. Therm. Eng. 12 (2018) 636–643, https://doi.org/10.1016/j.csite.2018.08.005.

[30] L. Zhao, K. Yu, W. Wu, Y. He, H. Dong, J. Wang, Effects of elastic micropillar array on the hydrothermal characteristics of a microchannel heat sink, Therm. Sci. Eng. Prog. 46 (2023) 102223, https://doi.org/10.1016/j.tsep.2023.102223.

[31] T. Saravanakumar, S. Kumar, D, Heat transfer study on different surface textured pin fin heat sink, Int. Commun. Heat Mass Transfer 119 (2020) 104902, https://doi.org/10.1016/j.icheatmasstransfer.2020.104902.

[32] H. Yan, L. Luo, J. Zhang, W. Du, S. Wang, D. Huang, Flow structure and heat transfer characteristics of a pin-finned channel with upright/curved/inclined pin fins under stationary and rotating conditions, Int. Commun. Heat Mass Transfer 127 (2021) 105483, https://doi.org/10.1016/j.icheatmasstransfer.2021.105483.

[33] B. Bencherif, D. Sahel, R. Benzeguir, H. Ameur, Performance analysis of central processing unit heat sinks fitted with perforation technique and splitter inserts, ASME J. Heat Mass Transfer 145 (2022), https://doi.org/10.1115/1.4055815.

[34] M.K.U. Al-Karagoly, M. Ayani, M. Mamourian, S. Razavi Bazaz, Experimental parametric study of a deep groove within a pin fin arrays regarding fin thermal resistance, International Communications in Heat and Mass Transfer 115 (2020) 104615. https://doi.org/10.1016/j.icheatmasstransfer.2020.104615.

[35] Q. Zhu, R. Su, L. Hu, J. Chen, J. Zeng, H. Zhang, H. Sun, S. Zhang, D. Fu, Heat transfer enhancement for microchannel heat sink by strengthening fluids mixing with backward right-angled trapezoidal grooves in channel sidewalls, Int. Commun. Heat Mass Transfer 135 (2022) 106106, https://doi.org/10.1016/j.icheatmasstransfer.2022.106106.

[36] B. Bencherif, D. Sahel, H. Ameur, R. Benzeguir, Investigation of the hydrothermal enhancement of grooved pin fins heat sinks, Int. J. Ambient Energy 43 (2022) 8505–8515, https://doi.org/10.1080/01430750.2022.2101521.

[37] H.-C. Chiu, R.-H. Hsieh, K. Wang, J.-H. Jang, C.-R. Yu, The heat transfer characteristics of liquid cooling heat sink with micro pin fins, Int. Commun. Heat Mass Transfer 86 (2017) 174–180, https://doi.org/10.1016/j.icheatmasstransfer.2017.05.027.

[38] M. Tabatabaei Malazi, K. Kaya, A.S. Dalkılıç, A computational case study on the thermal performance of a rectangular microchannel having circular pin-fins, Case Studies, Therm. Eng. 49 (2023) 103111, https://doi.org/10.1016/j.csite.2023.103111.

[39] Y.J. Lee, S.J. Kim, Experimental investigation on thermal-hydraulic performance of manifold microchannel with pin-fins for ultra-high heat flux cooling, Int. J. Heat Mass Transf. 224 (2024) 125336, https://doi.org/10.1016/j.ijheatmasstransfer.2024.125336.

[40] H.A.M. Hussein, R. Zulkifli, W.M.F.B.W. Mahmood, R.K. Ajeel, Effects of design parameters on flow fields and heat transfer characteristics in semicircle oblique-finned corrugated, International Communications in Heat and Mass Transfer 135 (2022) 106143. https://doi.org/10.1016/j.icheatmasstransfer.2022.106143.

[41] M. Abuška, V. Çorumlu, A comparative experimental thermal performance analysis of conical pin fin heat sink with staggered and modified staggered layout under forced convection, Therm. Sci. Eng. Prog. 37 (2023) 101560, https://doi.org/10.1016/j.tsep.2022.101560.

[42] E. Rasouli, C. Naderi, V. Narayanan, Pitch and aspect ratio effects on single-phase heat transfer through microscale pin fin heat sinks, Int. J. Heat Mass Transf. 118 (2018) 416–428, https://doi.org/10.1016/j.ijheatmasstransfer.2017.10.105.

[43] D. Yang, Y. Wang, G. Ding, Z. Jin, J. Zhao, G. Wang, Numerical and experimental analysis of cooling performance of single-phase array microchannel heat sinks with different pin-fin configurations, Appl. Therm. Eng. 112 (2017) 1547–1556, https://doi.org/10.1016/j.applthermaleng.2016.08.211.

[44] Y.-T. Shen, Y.-H. Pan, H. Chen, W.-L. Cheng, Experimental study of embedded manifold staggered pin-fin microchannel heat sink, Int. J. Heat Mass Transf. 226 (2024) 125488, https://doi.org/10.1016/j.ijheatmasstransfer.2024.125488.

[45] Z. Shi, X. Lan, J. Cao, N. Zhao, Y. Cheng, Numerical study of variable density and height flow guided pin fin in an open microchannel heat sink, Int. J. Heat Mass Transf. 225 (2024) 125405, https://doi.org/10.1016/j.ijheatmasstransfer.2024.125405.

[46] G.-F. Xie, L. Zhao, Y.-Y. Dong, Y.-G. Li, S.-L. Zhang, C. Yang, Hydraulic and thermal performance of microchannel heat sink inserted with pin fins, Micromachines 12 (2021) 245, https://doi.org/10.3390/mi12030245.

[47] A. Koşar, Y. Peles, Thermal-hydraulic performance of MEMS-based pin fin heat sink, J. Heat Transfer 128 (2005) 121–131, https://doi.org/10.1115/1.2137760.

[48] H. Shafeie, O. Abouali, K. Jafarpur, G. Ahmadi, Numerical study of heat transfer performance of single-phase heat sinks with micro pin-fin structures, Appl. Therm. Eng. 58 (2013) 68–76, https://doi.org/10.1016/j.applthermaleng.2013.04.008.
[49] S. Acharya, Thermo-fluidic analysis of microchannel heat sink with inline/staggered square/elliptical fins, Int. Commun. Heat Mass Transfer 147 (2023) 106961, https://doi.org/10.1016/j.icheatmasstransfer.2023.106961.
[50] H. Babar, H. Wu, H.M. Ali, W. Zhang, Hydrothermal performance of inline and staggered arrangements of airfoil shaped pin-fin heat sinks: A comparative study, Therm. Sci. Eng. Prog. 37 (2023) 101616, https://doi.org/10.1016/j.tsep.2022.101616.
[51] H. Kishore, C.K. Nirala, A. Agrawal, Thermal performance index based characterization and experimental validation for heat dissipation by unconventional arrayed micro pin-fins, Therm. Sci. Eng. Prog. 43 (2023) 102015, https://doi.org/10.1016/j.tsep.2023.102015.
[52] Experimental investigation of enhanced performance of pin fin heat sink with wings, Appl. Therm. Eng. 155 (2019) 546–562. https://doi.org/10.1016/j.applthermaleng.2019.03.139.
[53] F. Ismayilov, A. Akturk, Y. Peles, Systematic micro heat sink optimization based on hydrofoil shape pin fins, Case Stud. Therm. Eng. 26 (2021) 101028, https://doi.org/10.1016/j.csite.2021.101028.
[54] S. Singh, R.K. Singla, Experimental and numerical analysis of a nonlinear pin fin with temperature dependent properties and disparate boundary conditions, Int. Commun. Heat Mass Transfer 108 (2019) 104313, https://doi.org/10.1016/j.icheatmasstransfer.2019.104313.
[55] X. Cui, J. Guo, X. Huai, K. Cheng, H. Zhang, M. Xiang, Numerical study on novel airfoil fins for printed circuit heat exchanger using supercritical CO2, Int. J. Heat Mass Transf. 121 (2018) 354–366, https://doi.org/10.1016/j.ijheatmasstransfer.2018.01.015.
[56] L. Tang, L. Cui, B. Sundén, Optimization of fin configurations and layouts in a printed circuit heat exchanger for supercritical liquefied natural gas near the pseudo-critical temperature, Appl. Therm. Eng. 172 (2020) 115131, https://doi.org/10.1016/j.applthermaleng.2020.115131.
[57] M.R. Haque, R.R. Redu, M.-A.-A. Rafi, M.M. Haque, M.Z. Rahman, Numerical investigation of heat transfer performance for rectangular, elliptical, and airfoil shaped pin fin heatsinks through the novel combination of perforation and bulge inserts, Int. Commun. Heat Mass Transfer 138 (2022) 106352, https://doi.org/10.1016/j.icheatmasstransfer.2022.106352.
[58] Q. Shi, Q. Liu, X. Yao, C. Sun, X. Ju, M.M. Abd El-Samie, C. Xu, Optimal design on irregular polygon topology for the manifold micro-pin-fin heat sink, International Communications in Heat and Mass Transfer 141 (2023) 106574. https://doi.org/10.1016/j.icheatmasstransfer.2022.106574.
[59] R. Ray, A. Mohanty, P. Patro, K.C. Tripathy, Performance enhancement of heat sink with branched and interrupted fins, Int. Commun. Heat Mass Transfer 133 (2022) 105945, https://doi.org/10.1016/j.icheatmasstransfer.2022.105945.
[60] H. Ma, L. Su, B. He, D. He, Y. Kang, New design of U-turn type minichannel cold plate with hybrid fins for high temperature uniformity, Int. Commun. Heat Mass Transfer 135 (2022) 106078, https://doi.org/10.1016/j.icheatmasstransfer.2022.106078.
[61] E.M.S. El-Said, G.B. Abdelaziz, S.W. Sharshir, A.H. Elsheikh, A.M. Elsaid, Experimental investigation of the twist angle effects on thermo-hydraulic performance of a square and hexagonal pin fin array in forced convection, Int. Commun. Heat Mass Transfer 126 (2021) 105374, https://doi.org/10.1016/j.icheatmasstransfer.2021.105374.
[62] J.R. McDonough, A perspective on the current and future roles of additive manufacturing in process engineering, with an emphasis on heat transfer, Therm. Sci. Eng. Prog. 19 (2020) 100594, https://doi.org/10.1016/j.tsep.2020.100594.
[63] K. Timbs, M. Khatamifar, E. Antunes, W. Lin, Experimental study on the heat dissipation performance of straight and oblique fin heat sinks made of thermal conductive composite polymers, Therm. Sci. Eng. Prog. 22 (2021) 100848, https://doi.org/10.1016/j.tsep.2021.100848.
[64] P. Bhandari, K.S. Rawat, Y.K. Prajapati, D. Padalia, L. Ranakoti, T. Singh, Design modifications in micro pin fin configuration of microchannel heat sink for single phase liquid flow: A review, J. Storage Mater. 66 (2023) 107548, https://doi.org/10.1016/j.est.2023.107548.
[65] C. Woodcock, C. Ng'oma, M. Sweet, Y. Wang, Y. Peles, J. Plawsky, Ultra-high heat flux dissipation with Piranha Pin Fins, International Journal of Heat and Mass Transfer 128 (2019) 504–515, https://doi.org/10.1016/j.ijheatmasstransfer.2018.09.030.
[66] M. Harris, H. Wu, Numerical Simulation of Heat Transfer Performance in Novel Biomorphic Pin-Fin Heat Sinks, in: The 8th World Congress on Momentum, Heat and Mass Transfer, Avestia, Lisbon, Portugal, 2023. https://doi.org/10.11159/enfht23.166.
[67] S. Wu, K. Zhang, G. Song, J. Zhu, B. Yao, Experimental study on the performance of a tree-shaped mini-channel liquid cooling heat sink, Case Stud. Therm. Eng. 30 (2022) 101780, https://doi.org/10.1016/j.csite.2022.101780.
[68] Y. Xu, L. Li, J. Wang, Experimental and numerical investigations of the thermal–hydraulic characteristics of novel micropin-fin heat sinks, Int. J. Heat Mass Transf. 209 (2023) 124079, https://doi.org/10.1016/j.ijheatmasstransfer.2023.124079.
[69] M.A.A. Rehmani, S.A. Jaywant, K.M. Arif, Study of microchannels fabricated using desktop fused deposition modeling systems, Micromachines 12 (2021) 14, https://doi.org/10.3390/mi12010014.
[70] W. Wan, D. Deng, Q. Huang, T. Zeng, Y. Huang, Experimental study and optimization of pin fin shapes in flow boiling of micro pin fin heat sinks, Appl. Therm. Eng. 114 (2017) 436–449, https://doi.org/10.1016/j.applthermaleng.2016.11.182.
[71] J. Gao, Z. Hu, Q. Yang, X. Liang, H. Wu, Fluid flow and heat transfer in microchannel heat sinks: Modelling review and recent progress, Therm. Sci. Eng. Prog. 29 (2022) 101203, https://doi.org/10.1016/j.tsep.2022.101203.
[72] H. Ehsani, F.N. Roudbari, S.S. Namaghi, P. Jalili, D.D. Ganji, Investigating thermal performance enhancement in perforated pin fin arrays for cooling electronic systems through integrated CFD and deep learning analysis, Results Eng. 22 (2024) 102016, https://doi.org/10.1016/j.rineng.2024.102016.
[73] E.M. Mihalko, A. Basak, Optimizing thermal performance of pin-fin arrays using Bayesian methods for turbine cooling, Int. J. Heat Mass Transf. 225 (2024) 125355, https://doi.org/10.1016/j.ijheatmasstransfer.2024.125355.
[74] A. Sikirica, L. Grbčić, L. Kranjčević, Machine learning based surrogate models for microchannel heat sink optimization, Appl. Therm. Eng. 222 (2023) 119917, https://doi.org/10.1016/j.applthermaleng.2022.119917.
[75] M. Harris, An investigation on engine mass airflow sensor production via TQM, TPM, and six sigma practices, Oper. Res. Forum 2 (2021) 61, https://doi.org/10.1007/s43069-021-00102-y.
[76] Z. Huang, Y. Hwang, R. Radermacher, Review of nature-inspired heat exchanger technology, Int. J. Refrig 78 (2017) 1–17, https://doi.org/10.1016/j.ijrefrig.2017.03.006.
[77] A. Mohammadi, A. Koşar, Review on Heat and Fluid Flow in Micro Pin Fin Heat Sinks under Single-phase and Two-phase Flow Conditions, Nanoscale Microscale Thermophys. Eng. 22 (2018) 153–197, https://doi.org/10.1080/15567265.2018.1475525.
[78] K. Sefiane, A. Koşar, Prospects of heat transfer approaches to dissipate high heat fluxes: Opportunities and challenges, Appl. Therm. Eng. 215 (2022) 118990, https://doi.org/10.1016/j.applthermaleng.2022.118990.
[79] B. Yousefi-Lafouraki, M. Rajabi Zargarabadi, B. Sunden, Aerothermal analysis of pulsed jet impinging on a flat surface with different pin configurations, International Communications in Heat and Mass Transfer 137 (2022) 106263. https://doi.org/10.1016/j.icheatmasstransfer.2022.106263.
[80] M. Harris, H. Wu, J. Sun, Investigating Heat Transfer and Flow Characteristics under Different Wall Heating Conditions in Novel Micro Pin-Fin Heat Sinks, in: 9th World Congress on Momentum, Heat and Mass Transfer (MHMT 2024), Avestia, London, 2024. https://doi.org/10.11159/enfht24.328.
[81] P. Gómez-Gálvez, P. Vicente-Munuera, A. Tagua, C. Forja, A.M. Castro, M. Letrán, A. Valencia-Expósito, C. Grima, M. Bermúdez-Gallardo, Ó. Serrano-Pérez-Higueras, F. Cavodeassi, S. Sotillos, M.D. Martín-Bermudo, A. Márquez, J. Buceta, L.M. Escudero, Scutoids are a geometrical solution to three-dimensional packing of epithelia, Nat. Commun. 9 (2018) 2960, https://doi.org/10.1038/s41467-018-05376-1.
[82] E.S. Menon, Transmission Pipeline Calculations and Simulations Manual, Gulf Professional Publishing, 2014.
[83] D. Li, Encyclopedia of Microfluidics and Nanofluidics, Springer Science & Business Media, 2008.
[84] W. Yuan, J. Zhao, C.P. Tso, T. Wu, W. Liu, T. Ming, Numerical simulation of the thermal hydraulic performance of a plate pin fin heat sink, Appl. Therm. Eng. 48 (2012) 81–88, https://doi.org/10.1016/j.applthermaleng.2012.04.029.
[85] M.Z.U. Khan, E. Uddin, B. Akbar, N. Akram, A.A. Naqvi, M. Sajid, Z. Ali, M. Y. Younis, F.P. García Márquez, Investigation of heat transfer and pressure drop in microchannel heat sink using Al2O3 and ZrO2 nanofluids, Nanomaterials (Basel) 10 (2020) 1796, https://doi.org/10.3390/nano10091796.
[86] S. Akhtar, J.C. Kurnia, T. Shamim, A three-dimensional computational model of H2–air premixed combustion in non-circular micro-channels for a thermo-photovoltaic (TPV) application, Appl. Energy 152 (2015) 47–57, https://doi.org/10.1016/j.apenergy.2015.04.068.
[87] M. Shim, M.Y. Ha, J.K. Min, A numerical study of the mixed convection around slanted-pin fins on a hot plate in vertical and inclined channels, Int. Commun. Heat Mass Transfer 118 (2020) 104878, https://doi.org/10.1016/j.icheatmasstransfer.2020.104878.
[88] A.A.A.A. Al-Rashed, A. Shahsavar, O. Rasooli, M.A. Moghimi, A. Karimipour, M. D. Tran, Numerical assessment into the hydrothermal and entropy generation characteristics of biological water-silver nano-fluid in a wavy walled microchannel heat sink, Int. Commun. Heat Mass Transfer 104 (2019) 118–126, https://doi.org/10.1016/j.icheatmasstransfer.2019.03.007.
[89] A. Al-Damook, J.L. Summers, N. Kapur, H. Thompson, Effect of Different Perforations Shapes on the Thermal-hydraulic Performance of Perforated Pinned Heat Sinks, 3 (2016).
[90] D.N. Cosenza, L. Korhonen, M. Maltamo, P. Packalen, J.L. Strunk, E. Næsset, T. Gobakken, P. Soares, M. Tomé, Comparison of linear regression, k-nearest neighbour and random forest methods in airborne laser-scanning-based prediction of growing stock, Forestry: an International Journal of Forest Research 94 (2021) 311–323, https://doi.org/10.1093/forestry/cpaa034.
[91] J. Cai, K. Xu, Y. Zhu, F. Hu, L. Li, Prediction and analysis of net ecosystem carbon exchange based on gradient boosting regression and random forest, Appl. Energy 262 (2020) 114566, https://doi.org/10.1016/j.apenergy.2020.114566.
[92] J. Brownlee, Ensemble learning algorithms with python: make better predictions with bagging, boosting, and stacking, Machine Learning Mastery (2021).
[93] Z. Wu, X. Chen, Y. Mao, E. Li, X. Zeng, J.-X. Wang, A deep learning algorithm with smart-sized training data for transient thermal performance prediction, Case Stud. Therm. Eng. 39 (2022) 102420, https://doi.org/10.1016/j.csite.2022.102420.
[94] P. Kosky, R. Balmer, W. Keat, G. Wise, Chapter 14 - Mechanical Engineering, in: P. Kosky, R. Balmer, W. Keat, G. Wise (Eds.), Exploring Engineering (Fifth Edition),

Academic Press, 2021: pp. 317–340. https://doi.org/10.1016/B978-0-12-815073-3.00014-4.
[95] G. Wang, F. Yang, K. Wu, Y. Ma, C. Peng, T. Liu, L.-P. Wang, Estimation of the dissipation rate of turbulent kinetic energy: A review, Chem. Eng. Sci. 229 (2021) 116133, https://doi.org/10.1016/j.ces.2020.116133.
[96] M. Awais, A.A. Bhuiyan, Heat transfer enhancement using different types of vortex generators (VGs): A review on experimental and numerical activities, Therm. Sci. Eng. Prog. 5 (2018) 524–545, https://doi.org/10.1016/j.tsep.2018.02.007.
[97] R. Bekkerman, M. Bilenko, J. Langford, Scaling up Machine Learning: Parallel and Distributed Approaches, Cambridge University Press, 2011.
[98] M. Harris, M. Ndiaye, P. Farrell, Integration of industry 4.0 and internet of things in the automotive and motorsports sectors: an empirical analysis, SAE Technical Papers 5079 (2020) 1–12, https://doi.org/10.4271/2020-01-5079.
[99] Z. Duan, G. Xie, B. Yu, P. Jin, Multi-objective topology optimization and thermal performance of liquid-cooled microchannel heat sinks with pin fins, Case Stud. Therm. Eng. 49 (2023) 103178, https://doi.org/10.1016/j.csite.2023.103178.
[100] M.R. Attar, M. Mohammadi, A. Taheri, S. Hosseinpour, M. Passandideh-Fard, M. Haddad Sabzevar, A. Davoodi, Heat transfer enhancement of conventional aluminum heat sinks with an innovative, cost-effective, and simple chemical roughening method, Therm. Sci. Eng. Prog. 20 (2020) 100742, https://doi.org/10.1016/j.tsep.2020.100742.
[101] R.J. MGlen, An introduction to additive manufactured heat pipe technology and advanced thermal management products, Therm. Sci. Eng. Prog. 25 (2021) 100941, https://doi.org/10.1016/j.tsep.2021.100941.